12-2021

Understanding the Chemical Structures of Polydopamine

Deborah Takyibea Okyere
University of Arkansas, Fayetteville

Understanding the Chemical Structures of Polydopamine

A thesis submitted in partial fulfillment
of the requirements for the degree of
Master of Science in Microelectronics-Photonics

by

Deborah Takyibea Okyere
Bachelor of Science in Biochemistry, 2013
University of Ghana

December 2021
University of Arkansas

This thesis is approved for recommendation to the Graduate Council.

_____
Jingyi Chen, Ph.D.
Thesis Director

_____
Yong Wang, Ph.D.
Committee Member

_____
Yuchun Du, Ph.D.
Committee Member

_____
Yanbin Li, Ph.D.
Committee Member

_____
Matthew Leftwich, Ph.D.
Ex-Officio Member

The following signatories attest that all software used in this thesis was legally licensed for use by Deborah Takyibea Okyere for research purposes and publication.

_____	_____
Ms. Deborah Takyibea Okyere	Dr. Jingyi Chen, Thesis Director

This thesis was submitted to http://www.turnitin.com for plagiarism review by the TurnItIn company's software. The signatories have examined the report on this thesis that was returned by TurnItIn and attest that, in their opinion, the items highlighted by the software are incidental common usage and are not plagiarized material.

_____	_____
Dr. Matthew Leftwich, Program Director	Dr. Jingyi Chen, Thesis Director

Abstract

Polydopamine (PDA) is described as a bioinspired polymer produced by a method involving the chemical oxidation of dopamine in a pH-dependent medium. It has been used for the functionalization of nanomaterials in diverse applications including drug delivery and biosensing because of its strong adhesiveness, functionality is easily modified, and biocompatibility with mammalian cells and tissues. The polymerization process is believed to be initiated by the autoxidation of dopamine to dopaminequinone. However, the repeating units, as well as the final structure of PDA, are not well understood. Hence, this work focuses on the characterizations of the PDA structures during formation and degradation under different conditions to understand how the structures affect the PDA properties and functionality.

A commonly used method was chosen for the study of the PDA formation process. The synthesis of PDA was conducted in tris buffer at pH 8.5. Different microscopic and spectroscopic tools were utilized to characterize the morphology and chemical structures of the dopamine polymerization process. The results indicate that the PDA repeating units consist of dopamine, 5,6-dihydroxyindole, and indole-5,6 quinone. These repeating units are covalently bonded together forming different degrees of oligomers. Additionally, the tris base might be incorporated in the oligomers that form the PDA structure. To study the stability of the PDA structures, the degradation of the PDA was performed in hydrogen peroxide over a period of time. The resulting products mainly contain dimer and trimer units of the PDA structures that are water-soluble. Finally, the PDA formation process was used to modify the surface of silica and their subsequent use for the synthesis of metal-silica composite materials.

Acknowledgment

I thank God Almighty for His faithfulness throughout this work and in all spheres of life. Sincere gratitude goes to my supervisor, Dr. Jingyi Chen for her love, guidance, and patience throughout this study.

I also want to give special thanks to Dr. Rick Wise for his advice and guidance throughout my study. Heartfelt appreciation to Dr. Leftwich and Renee Jones-Hearon for always being there to support and help every step of the way.

To all members of the research group, thank you all for the diverse contributions towards the course of my study. I am very grateful to you all.

I am very grateful to Dr. Rohana Liyanage, for the help in generating mass spectrometry data and its interpretation. I also want to thank all the committee members for their immense support throughout this journey.

I would also like to thank my family for their immense support and prayers always. To my husband, I am very grateful for the encouragement and support throughout this journey.

This project is financially supported by National Science Foundation CMMI under Grant No.1563227 and the Center for Advanced Surface Engineering from NSF EPSCoR OIA Grant No.1457888. Any opinions, findings, and conclusions, or recommendations expressed in this material are those of the author and do not necessarily reflect the views of the National Science Foundation.

Dedication

This work is dedicated to the Lord God Almighty for His abundant grace and mercy and to my beloved family who has been my support and believed in me throughout this journey.

Table of Contents

List of Figures

List of Tables

1 Introduction

1.1 Background and Applications of Polydopamine

Polydopamine (PDA) is described as synthetic eumelanin. This eumelanin is natural melanin commonly found in living organisms. For example, in humans, the eumelanin is found in hair, skin, and eyes and functions as the main factor for determining the color of these organs in the body.[1] Polydopamine is described as synthetic eumelanin because it possesses similar physiochemical properties to eumelanin.[2] However, PDA structurally differs from eumelanin because it does not have the indole units that have been carboxylated (5,6-dihydroxyindole-2-carboxylic acid) as part of its building blocks.[2] It is formed via the self-polymerization of dopamine under basic conditions and in the presence of oxygen. The most common property possessed by PDA is its adhesiveness[3-5] which makes it possible to coat diverse surfaces for varying applications ranging from drug delivery to water purification systems.[6-9] PDA ability to form an adhesive polymer that coats different type of surface is as a result of functional groups like catechol found in amino acids such as 3,4-dihydroxy-L-phenylalanine (DOPA) and amine functional groups as found in amino acids like lysine.[6] Also, the PDA structure is made up of benzene rings, and therefore charged carriers can move throughout the pi system and this explains the ability of PDA to conduct electricity and its usage in organic electronics.[10, 11] The free radical scavenging ability of PDA is employed to thermally stabilize polymers such as poly(methyl methacrylate) (PMMA) whose degradation routes are well documented.[12] Fluorescence PDA is also designed in the form of capsules for drug delivery.[13, 14] These properties among others explain the multifunctional ability of PDA and its rapid emergence in fields such as material science, biomedicine, and energy conversion.[6, 7, 15, 16] Despite the great

insight into its usage and the mechanism of its formation, the structure of the final product are not well established. Yet, knowing the chemical structure of PDA plays a vital part in defining the relationship that exists between the structure, property, and function of the compound.

1.2 Synthesis of Polydopamine

Notwithstanding the great insight into PDA usage and the mechanism of its formation, the structure of the product is not well established. There are several proposals on the synthesis of PDA and pathways leading to its formation.[17-19] Nevertheless, in general, the synthesis of PDA varies with the concentration of dopamine HCl, type of buffer, pH, temperature, and duration used. These conditions do impact the yielded amount and properties exhibited by the resulting PDA. For example, PDA synthesis using dopamine HCl (1.0 g, 5.3 mmol) in 500 mL of water buffered with tris base (0.3 g, 2.5 mmol) and with a reaction time of 24 h at room temperature gave a product of 0.0873 g representing 11 % PDA[18] while a synthesis initiated by use of dopamine HCl (30 mg) reacted with bicarbonate buffer (0.1 M, pH=9) or tris buffer (0.05, pH=8.5) and under the same condition as the first synthesis described produced 28 % PDA.[2] Other PDA syntheses conducted using tris and phosphate buffers for a reaction time of 20 h obtained a higher yield from the tris buffer than the phosphate buffer. However, analysis of these products revealed that preparation parameters do not significantly affect the properties of the as-prepared PDA. Nonetheless, the size of the growing PDA is affected by the type of buffer used and depending on the ionic strength existing between the buffer and the polymer being formed, aggregation of particles in solution can be observed.[20] These differences account for the existence of different types of bond interaction in PDA, properties, and functionality of the as-prepared PDA.

1.2.1 Effect of Dopamine HCl Concentration on PDA Synthesis

The concentration of dopamine HCl used as starting material impacts the yield of the repeating units of the PDA being synthesized. Studies have shown that, decreasing the concentration of precursor used increases the product yield of PDA.[19] In terms of average particle size of PDA, mass concentrations of the precursor at 2 g/L and beyond, results in PDA aggregation in solution.[20, 21]

1.2.2 Effect of Buffer Type on PDA Synthesis

The type and concentration of buffer used also impact the size and yield of synthesized PDA. The mean diameter of synthesized PDA is impacted by the type of buffer used. Research has shown that larger particle sizes of PDA are obtained when phosphate buffer is used as opposed to the use of tris or sodium bicarbonate buffer.[20]

1.2.3 Effect of Oxidant on PDA Synthesis

Atmospheric oxygen is usually used as the oxidant for dopamine polymerization to form PDA. However, recent discoveries have shown that other oxidants in the form of salt, such as sodium periodate and sodium chlorate as well as metal ions such iron (III) and Cu (II), can be used to speed up the rate of PDA formation.[22-26] The use of different oxidants also affects the optical and colloidal property such as the size of the PDA particles formed.[27]

1.2.4 Proposed Pathway for the Formation of PDA

The path for the formation of PDA is generally accepted to be initiated by dopamine oxidation in the presence of buffer and oxygen. Also, in an anaerobic medium, the PDA

synthesis can be achieved by the use of oxidizing transition metal ions such as Fe^{3+} which speeds up the reactions at slightly acidic pH.[22] This synthesis can be tracked using the change in color of the solution from colorless to dark brown which finally becomes opaque.[20, 21] Now, to help in better understanding of the formation of PDA and behavior in different environments, different analytical techniques and methods have been employed in the studying of the structure of PDA. These techniques do not work in isolation but have been collectively used for the characterization of PDA. The subsequent sections focus on how these techniques have been used to examine the chemical structures of PDA.

The ultraviolet-visible (UV-Vis) spectroscopy is usually used to understand the underlying changes in the absorption spectrum as the PDA is being formed. Dopamine, with a similar structure as tyrosine, absorbs light at 280 nm and, during the PDA formation, aggregation does occur thus causing a red shift in absorption to higher wavelengths.[28] Yet, depending on the condition of preparation of PDA, a strong absorption peak can be observed in the ultraviolet range at 280 nm with no peak observed in the visible region.[19] A comparative study of the synthesized PDA and 5,6 dihydroxyindole (DHI) showed a single broad band spectrum in the UV-Vis region with higher absorption observed in the ultraviolet spectrum. This is said to be due to chemical disorder which is a distinct feature of both naturally occurring and synthetic eumelanin materials, but their functionality involving the coating of other surfaces differ.[2, 8]

Another important technique employed in PDA structure analysis is Fourier transform infrared (FTIR) spectroscopy. This technique is used to identify functional groups present in dopamine and PDA and how they differ from each other. For example, in dopamine spectrum peaks such as 1190 cm^{-1} and 1342 cm^{-1} corresponding to C-O and CH_2, respectively, can be identified. However, during the polymerization process, which involves some intra-cyclization,

some of these peaks are no longer observed in the FTIR spectrum obtained for PDA.[29] Hence, the transformation of dopamine to PDA is accompanied by a peak at 1515 cm^{-1} associated with N-H vibrations while a peak at 1605 cm^{-1} corresponds to an overlap of N-H bending and conjugated C=C vibrations in the aromatic ring as found in indole or indoline derivatives.[18, 30-32] Also, a more significant change between the dopamine spectrum and that of PDA is the change in frequency of N-H bonds observed when the amino group on the dopamine structure is converted to cyclized amine upon the intramolecular cyclization step in the PDA formation. The spectral changes observed in relation to amine cyclization are noticed between 3200 cm^{-1} and 2250 cm^{-1}. Other associated bands identified include 2433 cm^{-1}, 2539 cm^{-1}, 2638 $cm^{-1,}$ and 2748 cm^{-1}.[29] It is important to note the type of buffer used in PDA synthesis does not impact the functional groups identified in PDA.[33]

Another technique used in structural analysis of PDA is x-ray photoelectron spectroscopy (XPS). This technique helps confirm some structural elements and functional groups present in PDA. The most analyzed elements in PDA are carbon (C), oxygen (O), and nitrogen (N). The binding energies assigned to C-H (284.4 eV), C-N/C-OH (285.6 eV), and C=O (287.5 eV) are usually used to fit the C 1s spectrum. On the other hand, the peak at 532.4 eV is assigned to oxygen and is from the catechol and quinone functional groups of dopamine. Binding energy at 399.4 eV is usually associated with N 1s spectrum and is from amine, N-H of dopamine. [13, 32-34] The ratios of N/C and O/C experimentally obtained are compared to theoretical values of pure dopamine which are 0.125 and 0.250, respectively, to confirm the success of dopamine polymerization to form PDA.[6, 33] The analysis of these bonds is used to confirm the presence of functional groups in the formed PDA. For example, in a high pH environment, an increase of C=O percentage is used to denote the presence of more quinone groups in the formed PDA.[34]

The above techniques among others used in analyzing the structure of PDA are to aid in constructing the chemical structure of PDA based on the mass to charge ratio (m/z) of peaks generated from the mass spectrometer. The very first time the structure of PDA was analyzed using time-of-flight secondary ion mass spectrometry (TOF-SIMS) which only analyzed the surface of the structure of interest revealed that PDA consists of dihydroxyphenyl structures.[6] For in-depth structural information, other mass spectrometry techniques involve the use of laser desorption ionization mass spectrometry (LDI-MS) or electrospray ionization mass spectrometry (ESI-MS) is employed. The peak patterns generated from mass spectrometer are distinct from sample to sample owing to varying conditions under which PDA is synthesized. Yet, some peak patterns are similar in different patterns generated.[2, 19] In contradiction to this varying effect of synthesis conditions to PDA formation, there are other opposing views suggesting that varying dopamine concentration or changing the buffer type does not have any effect on the mass spectrometry peaks patterns generated.[21, 28] Some proposed structures of PDA in literature based on the techniques described above together with mass spectrometry technique include $(dopamine)_2$ or DHI held together by non-covalent bonds such as hydrogen bonds[35] and DHI, indoledione, and dopamine units held together by covalent bonds[33].

Even though the final structure of PDA is still not well understood, the intermediates leading to the final are well established. The route of the PDA synthesis is similar to that of eumelanin. The difference existing between the two synthesis pathways is how the reaction is initiated. For the biological reaction, tyrosine enzyme is required for the induction of the synthesis, but initiation of chemical reaction is spontaneous (Figure 1.1).[7] The first intermediate to be formed in the pathway is dopaminequinone which is a result of deprotonating and oxidation of the two catechol functional groups found in dopamine when placed in a basic medium.

Subsequently, the amino-functional group is also deprotonated and allows for intramolecular cyclization through chemical reaction referred to as 1,4-Michael addition. The intramolecular cyclization results in the formation of five-membered ring leading to the development of the next intermediate structure which is leukodopaminechrome. The remaining intermediates which are formed are due to the further oxidation and molecular rearrangement within the structures to form building units such as indolequinone and DHI.[7, 22, 35] However, controversies surround the use of DHI as the building block for the formation of PDA structure as the use of DHI as the precursor for PDA formation resulted in varied products in comparison to the use of dopamine HCl as the precursor for the PDA formation.[2]

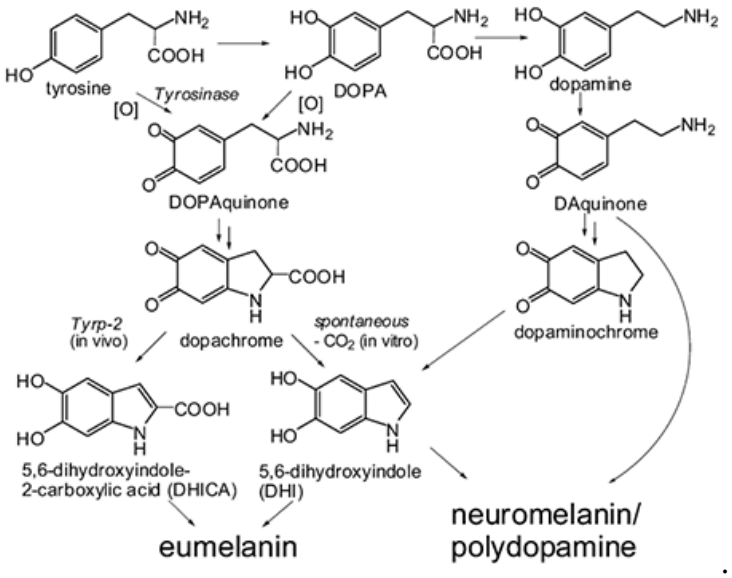

Figure 1.1 Schematic illustration for the synthesis of eumelanin and PDA (Reproduced with permission from reference[7]).

In terms of bonding interaction, the PDA formation process is described to have generated from two pathways: the first pathway being the oxidative polymerization via covalent bonding between the building units while the second pathway is self-interaction between the building units. The self-interaction is portrayed as non-covalent interaction.[35] On the contrary,

other studies suggest that both covalent and non-covalent forces contribute relatively equally to PDA formation. This statement is buttressed with the fact that during PDA polymerization, the interaction between monomer-monomer and monomer-oligomer is driven by covalent bonding while the stages of the polymerization are driven by non-covalent interaction to progressively grow into the complex structure of PDA.[21] Also, the formation of dopamine quinone has been found to play a key role in the formation of the PDA polymer. The role of dopamine quinone is divide into three pathways: 1) when a high concentration of dopamine is used, uncyclized dopamine forming dimers are formed as major intermediate steps; 2)when a low concentration of dopamine are involved, DHI is formed as a result of intramolecular cyclization as major intermediate steps; and 3) a mixture of intermediates proposed in pathways 1 and 2 are formed and any of these pathways may lead to the formation of cyclized dihydroxyindole derivatives, uncyclized catecholamine/quinones, and unidentified pyrrolecarboxylic acid units as building units of PDA.[19]

Another way researchers have tried to study the structure of polydopamine is to degrade the fully synthesized PDA with hydrogen peroxide in an alkaline medium. This degradation study proposes the building units of PDA as pyrrolearboxylic acid units, uncyclized catecholamine, and cyclized DHI units.[19] Under the same reaction medium, others have proposed that under alkaline conditions, hydrogen peroxide breaks down into hydroxyl radicals to mediate the breakdown of PDA to form fluorescent polydopamine dots.[36] Another study has shown that in the absence of hydrogen peroxide, PDA degradation can be induced by adjusting the basic conditions to pH greater than 11 to form smaller building units of PDA that are soluble in water.[37] However, just like with the PDA formation, the mechanism of degradation and final degraded products is still not clear.

One main application of dopamine is surface modification. The identification of dopamine as a suitable material for all types of surfaces was inspired by the mussels that secrete adhesive proteins for attachment to solid surfaces under marine water. These adhesive proteins are known as *Mytilus edulis* foot protein 5 (Mefp-5) and are found near the byssal foot of the mussels. The adhesive protein possesses ninety-nine amino acids, of which twenty-eight of them are 3,4-dihydroxy-L-phenylalanine (DOPA) and lysine is also in relative abundance. These amino groups contain the catechol functional group (DOPA) which is obtained from the hydroxylation of tyrosine and amine functional group ($-NH_2$) from lysine. These functional groups play vital roles in helping the mussel foot bind to solid surfaces under marine water. Dopamine identified as a suitable material for surface modification imitates this adhesive protein because it has both the catechol and amine functional group present as part of its building unit.[6]

The use of spectroscopic tools described above among others under different conditions have helped to gain insight into proposed PDA structures and mechanism of synthesis. Nonetheless, the mystery surrounding its structure remains unresolved. Hence, a more profound method which involves a well-controlled chemical reaction for the synthesis and tracking its formation and degradation with respect to time can provide new information to aid in better understanding the chemical structure and nature of PDA.

1.3 Objective

The objective of this work was to understand the formation and degradation of polydopamine. In this work, the formation of polydopamine was understudied via time course study to identify the repeating units in PDA and how structure increased in size with respect to time. In addition, the as-synthesized PDA is degraded using 50 % hydrogen peroxide under a

time course study, and the degraded products were analyzed using spectroscopic tools such as mass spectrometry. These identified degraded products were compared with the building units identified in the PDA formation to gain a better understanding of nature and identify repeating units of the PDA. Finally, the use of PDA for surface modification and as an intermediate layer for coating one nanoparticle over another were explored in this work.

2 Experimental Methods

2.1 Chemicals and Materials

Tris-(hydroxymethyl) aminomethane (Trizma base, >99%), Dopamine hydrochloride (DA, 99%), tetraethyl orthosilicate (TEOS), ammonium hydroxide (28.0 -30.0 % NH_3), formic acid, sodium citrate, potassium chloride and α-cyano-4-hydroxycinnamic purchased were purchased from Sigma-Aldrich (St. Louis, MO). Acetic Acid, sodium ascorbate, and silver nitrate (99.9 %) were purchased from Alfa Aesar (Ward Hill, MA). Sodium borohydride ($NaBH_4$) was purchased from Fluka (Buchs, Switzerland). Ethanol (100%) was purchased from Koptec (King of Prussia, PA). Ascorbic acid was purchased from BDH (Poole, United Kingdom). Deuterium oxide (D_2O, 99.9%) was purchased from Cambridge Isotope Laboratories, Inc., (Tewksbury, MA). Hydrogen peroxide (H_2O_2, 50% solution) was purchased from Acros Organics (Geel, Belgium). Peptide calibration standard II was purchased from Bruker Daltonics (Billerica, MA). 18 MΩ H_2O was used in the performance of all the experiments unless otherwise stated. All chemicals were used as received.

2.2 Synthesis

2.2.1 Synthesis of Polydopamine (PDA)

Polydopamine was prepared by self-polymerization of dopamine HCl under basic conditions and at room temperature.[38] Reaction was performed in a 250 mL beaker equipped together with a dispenser (IKA T 18 digital ULTRA-TURRAX) furnished with dispersing element (IKA S 18 N-10 G). To begin with, Trizma base (2mmol, 0.242 g) was dissolved in 200 mL of water with continuous stirring at a speed of 2800 rpm for 5 min. Dopamine HCl (0.6 g)

was then added to the basic solution and the reaction was allowed to run for 24 h under continuous exposure to the atmosphere. The dispersing speed of 2800 rpm was kept constant throughout the process. The product obtained was quenched by the addition of 2 mL of acetic acid (1 % volume of the reaction mixture). The acidified product was centrifuged at 8400 rpm for 15 min and further purified with water thrice at 14000 rpm for 15 min at 4 °C. The final product was redispersed in water and freeze-dried for further characterization.

2.2.2 Time Course Study of PDA Synthesis

The PDA formation was monitored for 24 h. However, a volume of 1 mL was sampled out at the following time points: 0.5, 30, 60, 300, 1080, and 1440 min. These samples were quenched by the addition of 10 μL of acetic acid and subjected to matrix-assisted laser desorption-ionization (MALDI) analysis.

2.2.3 Degradation of PDA

The mass of the solid PDA product after freeze-drying was obtained and dissolved in 50 % H_2O_2 (13 mL) to make a solution with a concentration of 10 mg/mL. The reaction was allowed to run for 2 days after which about 10 mg was aliquoted to be freeze-dried. Subsequently, 10 mg of aliquots were collected and freeze-dried after 4 days, 8 days, and 30 days respectively. These freeze-dried samples were dissolved in water or D_2O for further characterization.

2.2.4 Synthesis of Silica Nanoparticles

Silica nanoparticles were synthesized by mixing tetraethyl orthosilicate (TEOS), ethanol, water, and ammonium hydroxide in a molar ratio of 1:75:31:4. The reaction mixture was stirred for 3 h at room temperature. After 3 h, the resulting mixture was centrifuged at 10,000 rpm for 10 min and washed three times with water at 10,000 rpm and for 10 min. The resulting product was air-dried overnight and ready for use.

2.2.5 Synthesis of SiO_2-PDA Core-shell Nanoparticles

Water of volume 40 mL was heated to 50 °C and dispersed at a speed of 2800 rpm. Trizma base (0.0484 g) was then added to the beaker of water and allowed to dissolve for 5 min. After 5 min, 1 mL of the synthesized silica was added to the solution and allowed to dissolve for 5 min. Finally, 0.253 g of dopamine HCl was added to the reaction mixture and the reaction was allowed to run for 60 min. The dispersing speed was maintained at 2800 rpm throughout the period. After 60 min, the dispenser and heat were turned off and the reaction mixture was transferred into 50 mL centrifuge tubes. These tubes were placed in an ice bath for about 15 min for the reaction to be quenched. The resulting product was centrifuged at 10,000 rpm for 10 min and washed twice with water at 14,000 rpm for 10 min. The final product was dispersed in water and ready for characterization.

2.2.6 Synthesis of SiO_2-PDA Core-shell Nanoparticles Coated with Silver (Ag) using $NaBH_4$

0.1 mL of SiO_2-PDA was transferred into a 10 mL round bottom flask and 1 mL of $AgNO_3$ (0.04 M) solution was added under continuous stirring. This was followed by the transfer of 9.1 mg of $NaBH_4$ to form a colloidal solution at room temperature. This formed as seeds for

the growth of silver nanoparticles. The solution was brought to boil and 0.5 mL of sodium citrate (0.34 M) was followed by the addition of 0.5 mL of $AgNO_3$ (0.15 M). The total reaction time was 15 min. The final product was washed twice with water at 6500 rpm for 10 min and dispersed in water for characterization.

2.2.7 Synthesis of SiO_2-PDA Coated with Ag using Sodium Citrate

0.1 mL of SiO_2-PDA was transferred into a 10 mL round bottom flask containing 2 mL of water and 1 mL of sodium citrate (0.34 M) was added to it. This was followed by the addition of 3 mL of $AgNO_3$ (0.15 M) at a rate of 0.2 mL/minute. The total reaction time was 15 min. The final product was washed twice with water at 6500 rpm for 10 min and dispersed in water for characterization.

2.2.8 Synthesis of SiO_2-PDA Coated with Ag using Sodium Citrate and $NaBH_4$

0.1 mL of SiO_2-PDA was transferred into a 10 mL round bottom flask containing 5 mL of water and 3 mL of 1 mM $AgNO_3$ solution was added to it. This was allowed to mix for 30 min after which 3 mL of sodium citrate (4.28 mM) was added to it. The reaction time was 15 min after which 2 mL of 2 mM $NaBH_4$ solution was added in a dropwise manner until there was a change of color to grayish yellow. The total reaction was about 2 h and the product was centrifuged at 11,000 rpm for 30 min. The final product was washed twice with water at 14,000 rpm for 15 min and dispersed in water for characterization.

2.2.9 Synthesis of PDA-Ag Core-Shell Nanoparticles using $NaBH_4$/ Sodium Citrate/ Ascorbic Acid/ Sodium Ascorbate

0.2 mL of PDA was transferred into a 50 mL round bottom flask containing 5 mL of water and 3 mL of 1 mM $AgNO_3$ solution was added to it at a rate of 0.2 mL/minute. The reaction mixture was allowed to mix for about 30 min after which 3 mL of 4.28 mM trisodium citrate solution/ 2 mL of 5 mM $NaBH_4$ / 2 mL of trisodium citrate / 2 mL of 5 mM ascorbic acid / 2 mL of 5 mM sodium ascorbate was added at fast injection and allowed to mix for 10 min. A total volume of 2 mL of 1 mM $AgNO_3$ was added at a rate of 0.2 mL/min. The reaction mixture was then allowed to run for 30 min. The resulting mixture was centrifuged at 11,000 rpm for 30 min. This was followed by purification with water twice at 14,000 rpm for 15 min. The final product was dispersed in water.

2.3 Characterization

2.3.1 UV-Vis Spectroscopy

Spectra of the samples were obtained using Agilent Cary 50 UV-Vis spectrophotometer (Agilent Technologies, Inc., Santa Clara, CA). A quartz cuvette was used for taking the spectra for the PDA samples. Depending on the concentration of the sample, ~ 25 μL was taken from the stock sample and diluted with 18 MΩ H_2O to record absorbance between 0.1 and 1.

2.3.2 Fourier-Transform Infrared (FTIR) Spectroscopy

KBr method was used to obtain the infrared spectra using an FTIR spectrometer. Samples prepared were made of 2 mg of analyte and 100 mg of KBr. The powdery sample was converted to a transparent pellet using a pellet press. The pellet formed was placed in an FTIR sample holder before analysis.

2.3.3 Transmission Electron Microscopy (TEM) Imaging

The samples were imaged using a JEOL JEM -1011 (JEOL USA, Inc., Peabody, MA) with an accelerating voltage of 100 kV. ImageJ was used to measure the particle size of the samples. Samples were prepared by diluting 10 μL of the sample with 18 MΩ H_2O in a ratio of 1 to 1. From this new prepared solution, 3 μL of the diluted sample was drop cast onto a Cu mesh grid and dried before imaging.

2.3.4 Dynamic Light Scattering (DLS) and Zeta Potential

The hydrodynamic diameter of the samples and surface charges were measured using a Brookhaven ZetaPALS dynamic light scattering instrument (Upton, NY). Samples for DLS measurements were prepared using 18 MΩ H_2O filtered with 2.2 μm nylon filter and the total volume of solution is 2 mL for each sample. The absorbance of these samples was then measured using UV-Vis spectrum to record an absorbance of 0.1. For zeta potential measurements, the samples were prepared using 1 mM KCl solution and a total volume of 1.5 ml was used for each measurement.

2.3.5 Nuclear Magnetic Resonance (NMR) Spectroscopy

The chemical structure of synthesized PDA (24 h sample) and all the degraded samples were examined using ^1H NMR on Bruker 400 MHz spectrometer (Billerica, MA). The spectra were obtained by dissolving 5 mg of each sample in 1mL of D_2O. These samples were subsequently transferred into 5 mm NMR tubes for analysis using an NMR spectrometer.

2.3.6 Matrix-Assisted Laser Desorption-Ionization time of flight (MALDI-TOF) Mass Spectrometry

The mass spectra of the PDA samples were obtained with matrix-assisted laser desorption-ionization time of flight (MALDI-TOF/TOF) mass spectrometer Bruker Ultraflex II (Billerica, MA) which functions in reflection mode. The MALDI-TOF spectrometer was operated using a 355 nm YAG laser. The laser position was moved around the spot randomly to collect ions from at least 500 laser shots which were then averaged to obtain spectra of the various samples being analyzed. A Bruker ground steel MTP 384 target plate was used for the preparation of the MALDI spots. Before spotting on the target plate, 0.1 % formic acid was used to prepare a saturated solution of α-cyano-4-hydroxycinnamic (HCCA) matrix and premixed with samples in the ratio of 1 to 1. These spots were then air-dried before being exposed to MALDI. A MALDI spot comprising of peptide calibration standard II was prepared in the same manner as the samples to be analyzed and was used to standardize the time of flight. Bruker Daltonics flex analysis 3.4 software was used to analyze the data obtained from MALDI.

3 Results and Discussion

3.1 PDA Formation

PDA is generally synthesized by exposing dopamine HCl to air in the presence of basic conditions such as tris base, pH 8.5. During this reaction, the catechol group present in the dopamine structure oxidizes to the quinone compound due to the presence of oxygen[39]. This oxidation is followed by polymerization to form the complex structure of PDA due to the presence of an aminoethyl functional group present in a basic solution.[39] The dopaminequinone formed is identified as the main control point for PDA formation: when the dopamine HCl concentration is high, dimerization of the uncyclized dopamine HCl is the major pathway, while at low dopamine HCl concentration, intramolecular cyclization of the dopaminequinone is the major pathway leading to the formation of the complex structure of PDA.[19] Among the factors that can be regulated in the PDA formation, buffer type seems to play a major role in the control of the PDA formation and properties of the synthesized PDA. Tris base was selected for this study to help fine-tune the size of the aggregate and properties of as-prepared PDA.[20] Also, in this study, instead of incubating the dopamine HCl in buffered solution over a period of time, an established dispersion method developed in this research group was used to achieve the fast formation of the polydopamine. To obtain optimum mixing of suspension, the disperser operates at a high circumferential speed which draws the reaction mixture spontaneously into the head of the dispersion. The reaction mixture which comes out radially via openings found between the stator and rotor designed is first pulled into the dispersion head (Figure 3.1).[38]

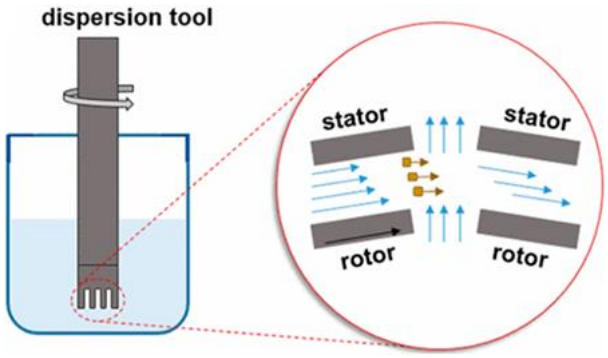

Figure 3.1 Graphical representation of dispersion method setup used for PDA formation with a focused view on the dispersion head showing the directional flow associated with it (modified from reference [38]).

The formation of PDA was monitored for 24 h during which the color change of reaction solution observed was from colorless to black precipitated solution. It is worthy to note that the preparation condition of PDA affects its structural properties. Previous studies[19] indicate that dopamine HCl with high a concentration (10 mM) shows a distinct band at 280 nm in the ultraviolet region with little or no absorbance in the visible indicating the presence of a high level of uncyclized dopamine HCl in the synthesized PDA. Yet, dopamine HCl with low concentration (0.5 mM) shows a less intense band at 280 nm with an undistinguishable absorption band in the visible region indicating the presence of low levels of dopamine and high levels of DHI as found in eumelanin-like compounds.[19] Conversely, in this study, PDA formation was monitored using the UV-Vis absorption spectrum. Comparing the absorbance of dopamine HCl (Figure 3.2A) to that of synthesized PDA (Figure 3.2B), it was observed that the absorption spectrum of dopamine showed a distinct absorbance peak at 280 nm but after oxidation and polymerization, PDA showed absorbance in both ultraviolet and visible regions due to the presence of DHI units. Even though a high concentration of dopamine HCl (15 mM) was utilized in this study, the intensity of the peak detected was broad and less intense which was contradictory to the result reported by Della Vecchia et al., 2013.[19] Also, a broad peak between 280 nm and 300 nm which

was less intense as compared to the peak detected for dopamine HCl indicated the presence of low levels of uncyclized dopamine in the synthesized PDA. The broadening of the peak and red shift observed in the PDA spectrum was due to an increase in the size of the PDA cluster formed as observed in the TEM image (Figure 3.3). Furthermore, the broadening of the absorbance spectrum of PDA that was observed was due to the existence of chemical disorder in PDA as exhibited in other eumelanin. The chemical disorder observed is a result of a mixture of oligomers with distinct chemical structures possessing different energy gaps present in eumelanin.[36, 40, 41]

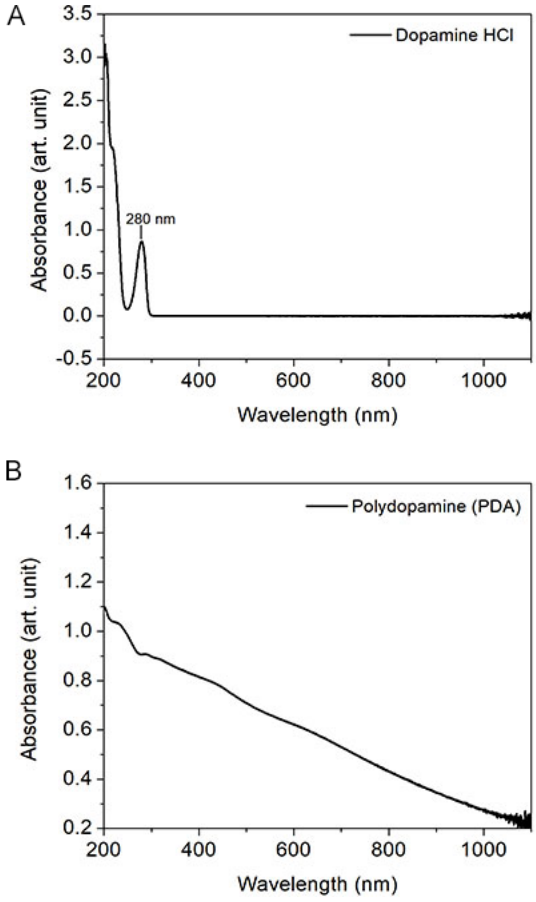

Figure 3.2 UV-Vis spectra of aqueous suspensions of different materials: (A) dopamine HCl; and (B) PDA synthesized by self-polymerization in tris buffer at pH=8.5.

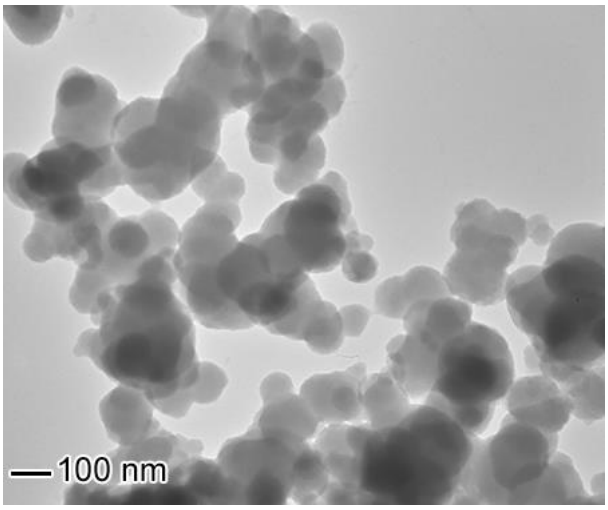

Figure 3.3 TEM characterization of PDA synthesized by self-polymerization in tris buffer at pH=8.5.

Establishing the fact that uncyclized dopamine HCl, as well as DHI, might be present in the formed PDA, FTIR analysis was carried out on dopamine HCl and synthesized PDA in order to identify the functional groups that support the UV-Vis results. Figure 3.4 displays the IR spectra of dopamine HCl and the synthesized PDA that were obtained by compacting the solid of the dopamine HCl and PDA with KBr powder to form a transparent pellet. Distinctive peaks associated with dopamine HCl that were identified included N-H stretching vibrations of primary amine (3372 cm^{-1}), N-H bending vibrations of primary amine (1612 cm^{-1}), O-H stretching related to intermolecular hydrogen bonding of the catechol group (3252 cm^{-1}), aromatic C-H stretch (3042 cm^{-1}) and aromatic ring stretch (1495 cm^{-1}). Upon oxidation and polymerization of dopamine HCl to form PDA, the FTIR spectrum indicated a broad band at 3420 cm^{-1}. This broad band formed was a characteristic of intermolecular O-H that exists between cyclized and uncyclized oligomers that constitute the complex structure of PDA. Also, underneath this broad band was the N-H stretch of secondary amine which are formed during the intramolecular cyclization of dopamine HCl via 1,4-Michael addition to form leucodopaminechrome which

readily oxidize to dopaminechrome. Other peaks identified in the PDA spectrum were 1612 cm^{-1} and 1495 cm^{-1} which were associated with aromatic ring stretching vibrations of the polyindole structures. Subsequently, in the initial stages of the PDA formation, there was a band at 1730 cm^{-1} that corresponds to carbonyl functional group (C=O) stretching vibration. This band tends to decrease relative to the polyindole ring stretch with a longer reaction time.[42] Hence, in a 24 h PDA reaction product, no band corresponding to the carbonyl group was identified. Theoretical analysis of the polymerization of PDA suggests that DHI and indole-5,6 quinone exist in equilibrium and can be converted to one form or the other during the polymerization.[43] Hence, depending on the duration of the PDA synthesis, it is possible to identify only the catechol form or the carbonyl form in the sample. The peak position in identified in Figure 3.4 is summarized in table 3.1.

Further probing of the structure of PDA was carried out by employing liquid state ^{1}H NMR spectroscopy using D_2O as solvent. The signals of the protons observed were multiplet (6.74-6.91 ppm) and two triplets of protons (2.85-3.24 ppm) (Figure 3.5B). A similar spectrum was obtained for proton NMR of dopamine HCl (Figure 3.6A). The signals of the aromatic protons were identified as multiplet (6.72-6.89 ppm) located at proton positions H3, H4, and H5 of the dopamine. Additionally, two triplets of methyl protons (2.83-3.22 ppm) located at proton positions H1 and H2 of the dopamine were also identified. These ^{1}H assignments correspond to literature values.[44-46] The similarities observed between the proton spectra of dopamine HCl, and synthesized PDA indicate that the aromatic ring found at the core of the dopamine HCl was retained in the synthesized PDA. This same observation was made in a previous study that employed solid-state ^{13}C NMR spectroscopy as the analytical tool. [18]

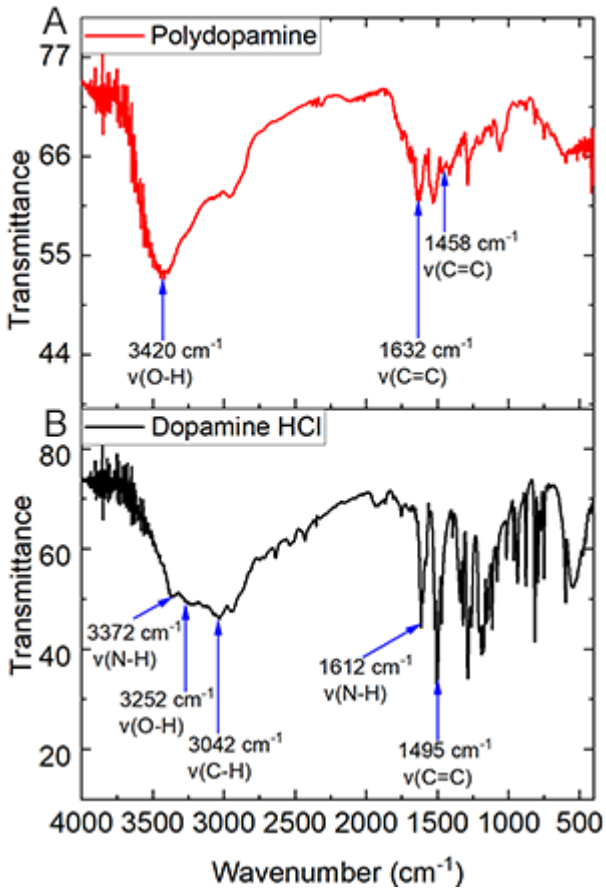

Figure 3.4 IR spectra of as-synthesized PDA (A); and dopamine HCl (B).

Table 3.1 Summary of peak position identified in the IR spectra shown in Figure 3.4

Dopamine HCl	Polydopamine (PDA)
N-H – 3372 cm^{-1}	O-H – 3420 cm^{-1}
O-H – 3252 cm^{-1}	C=C – 1632 cm^{-1}; 1458 cm^{-1}
C-H – 3042 cm^{-1}	
N-H – 1612 cm^{-1}	
C=C – 1495 cm^{-1}	

Also, since the spectra of the dopamine HCl were similar to that of the PDA, it supports the UV-Vis spectrum results of synthesized PDA in which it was observed that uncyclized dopamine might have been present in the synthesized PDA. Other peaks that were identified in the PDA spectrum but were absent in the dopamine HCl proton spectrum included 2.01 ppm corresponding to proton NMR for acetic acid and 3.24 ppm corresponding to proton NMR for tris base. The presence of the peak corresponding to the tris base indicates that the tris base may or may not have been incorporated into the PDA structure as previously reported.[19, 28] The incorporation of tris base in PDA samples during oxidation may be less or more pronounced in the formed PDA. The degree of incorporation of the tris base is dependent on the concentration of the dopamine HCl used as the starting material.[19]

A combination of the UV-Vis and NMR results suggests that uncyclized dopamine HCl, indole-5,6 quinone, or 5,6-dihydroxyindole units form part of the building blocks for the PDA. Previous research has suggested that pyrrolecarboxylic acid moieties[19] or dopaminechrome units[28] might also form part of the building block of the PDA. To establish the building unit forming the PDA, MALDI-TOF analysis was carried out to obtain more structural information from the synthesized PDA. The color changes observed during the time course of the PDA formation were subjected to mass spectrometry analysis. The analysis was carried out for samples labeled as control (dopamine HCl in water acidified with acetic acid), 0.5 min PDA, 30 min PDA, 60 min PDA, 300 min PDA, 1080 min PDA, and 1440 min PDA to track the formation of the PDA and how the repeating units increased with time. The resulting spectra observed indicated that the m/z of the PDA increased with a longer reaction time (Figure 3.6). From the analysis of the data, unreacted dopamine was detected m/z 154.1 and tris moieties at m/z 122 (Figure 3.6). The peaks corresponding to PDA formation suggest a combination of

uncyclized dopamine, indole-5,6 quinone, and 5,6-dihydroxyindole units via covalent bonding with the incorporation of tris moieties. Some identified peaks include trimer formation at m/z 438.2, 444.1, 446.1, and 448.1 (Figure 3.6). These peaks corresponded to a combination of a unit of uncyclized dopamine HCl to two units of indole-5,6 quinone or a unit of uncyclized dopamine HCl to two units of 5,6-dihydroxyindole covalently bonded together (Figure 3.7). The proposed structures for the peaks labeled with the numbers in blue in figure 3.6 were identified in Figure 3.7. Also, the peak at m/z 571.2 corresponded to a combination of one monomer of uncyclized dopamine HCl and two monomer units of 5,6-dihydroxyindole with incorporation tris moieties (Figure 3.7). A tetramer peak was identified at m/z 710.2 (Figure 3.6) corresponding to a combination of monomer unit of uncyclized dopamine HCl, monomer unit of 5,6-dihydroxyindole, and two monomer units of indole-5,6 quinone (Figure 3.7). Pentamer was identified at m/z 861.2 (Figure 3.6) suggesting a combination of one monomer of dopamine HCl to four monomers of 5,6-dihydroxyindole (Figure 3.7). These formed structures support reports that the formation of PDA in tris buffer can easily incorporate unreacted dopamine and tris moieties into the synthesized PDA.[19, 33, 35, 47] Consequently, the oligomers identified in this work support the report that the building units of PDA are linked covalently via the C-C bonds between the aromatic rings of the monomer units identified.[33]

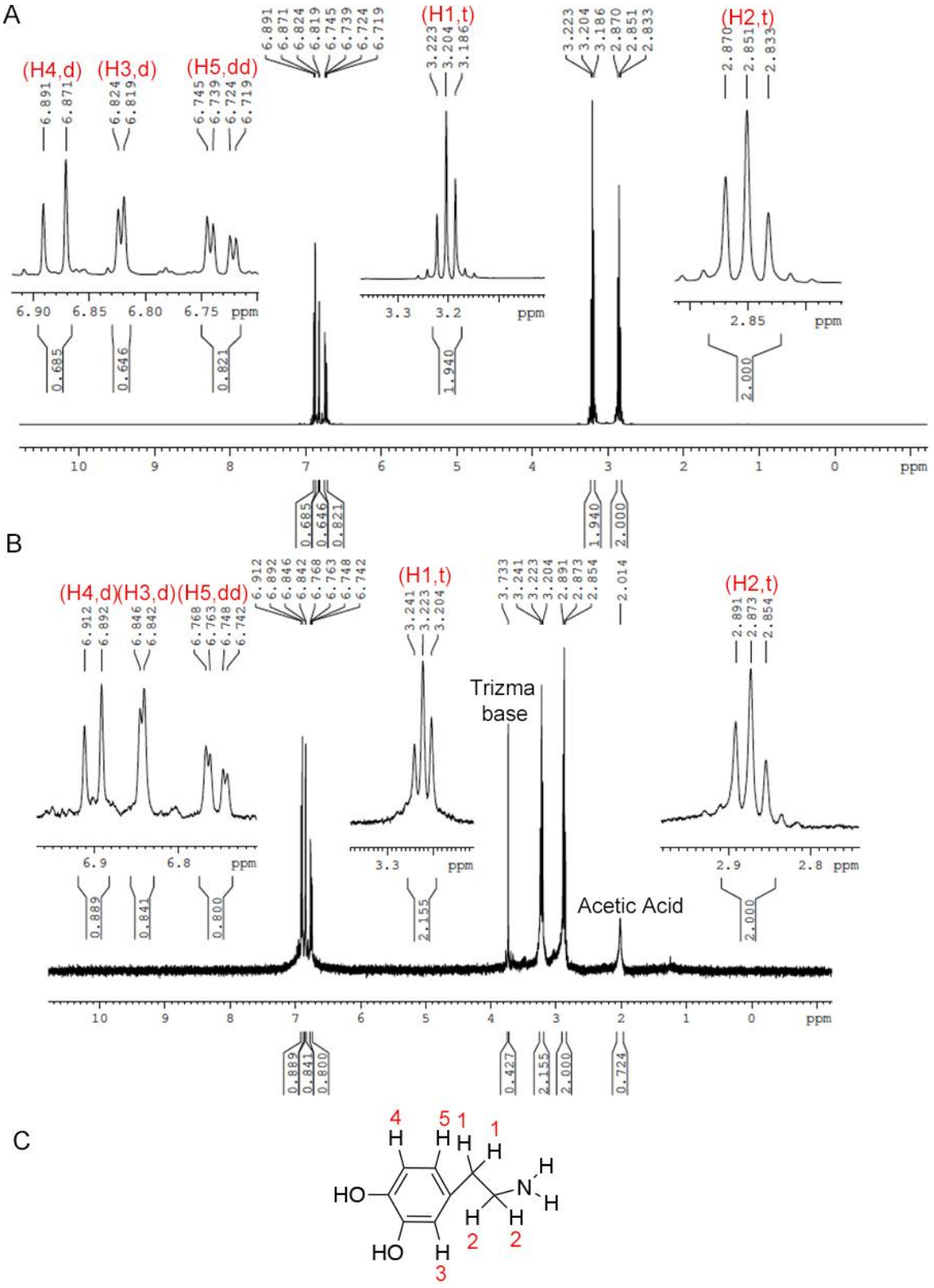

Figure 3.5 (A, B) ^{1}H NMR spectra of different materials in D_2O: (A) dopamine HCl, and (B) PDA. (C) Chemical structure of dopamine indicating ^{1}H assignments identified in NMR spectra.

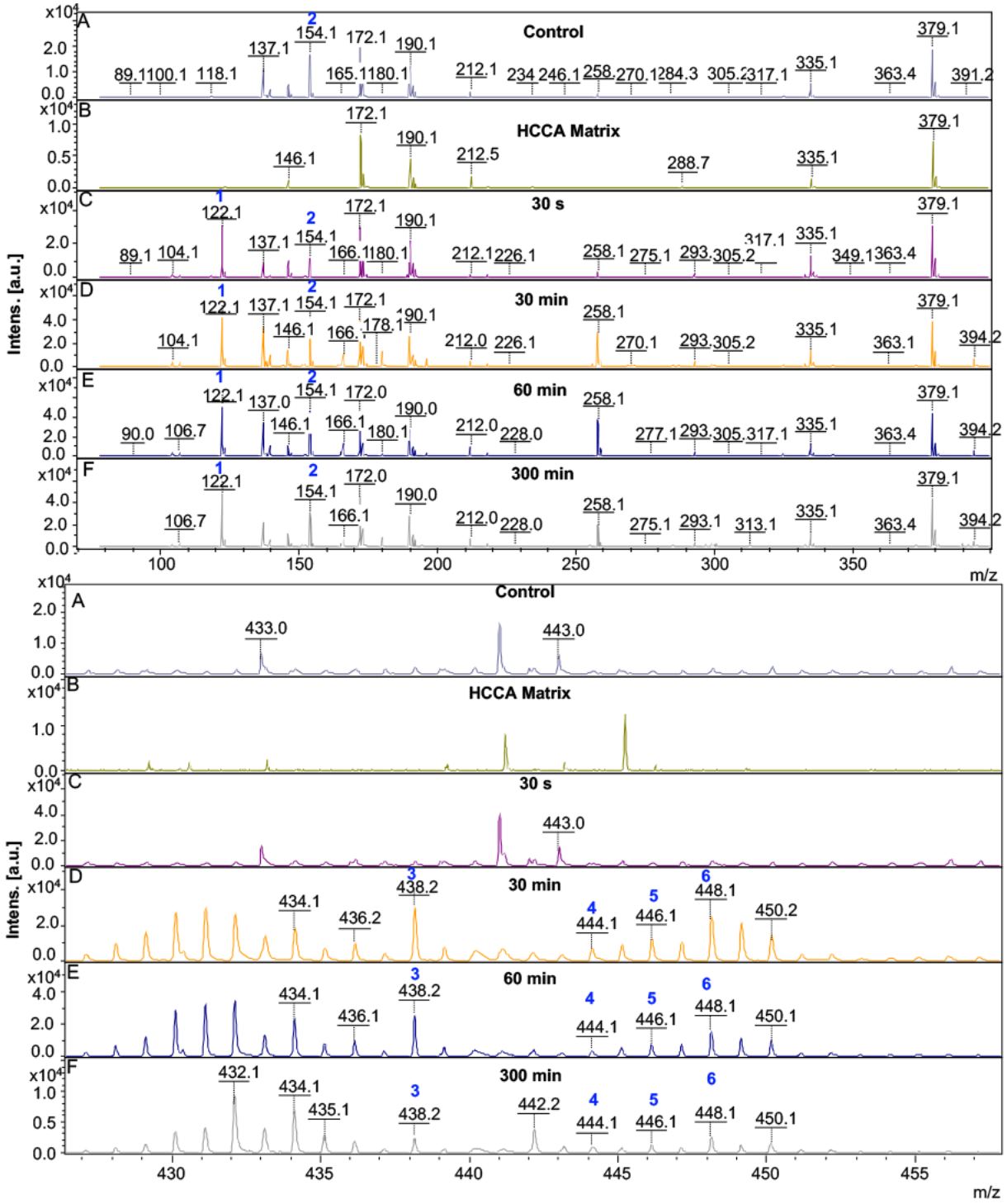

Figure 3.6 MALDI-TOF mass spectra of PDA formed during the time-course study: A) Control (aqueous dopamine HCl acidified with acetic acid); B) α-cyano-4-hydroxycinnamic acid (HCCA) matrix; C) 30 s; D) 30 mins; E) 60 mins; F) 300 mins.

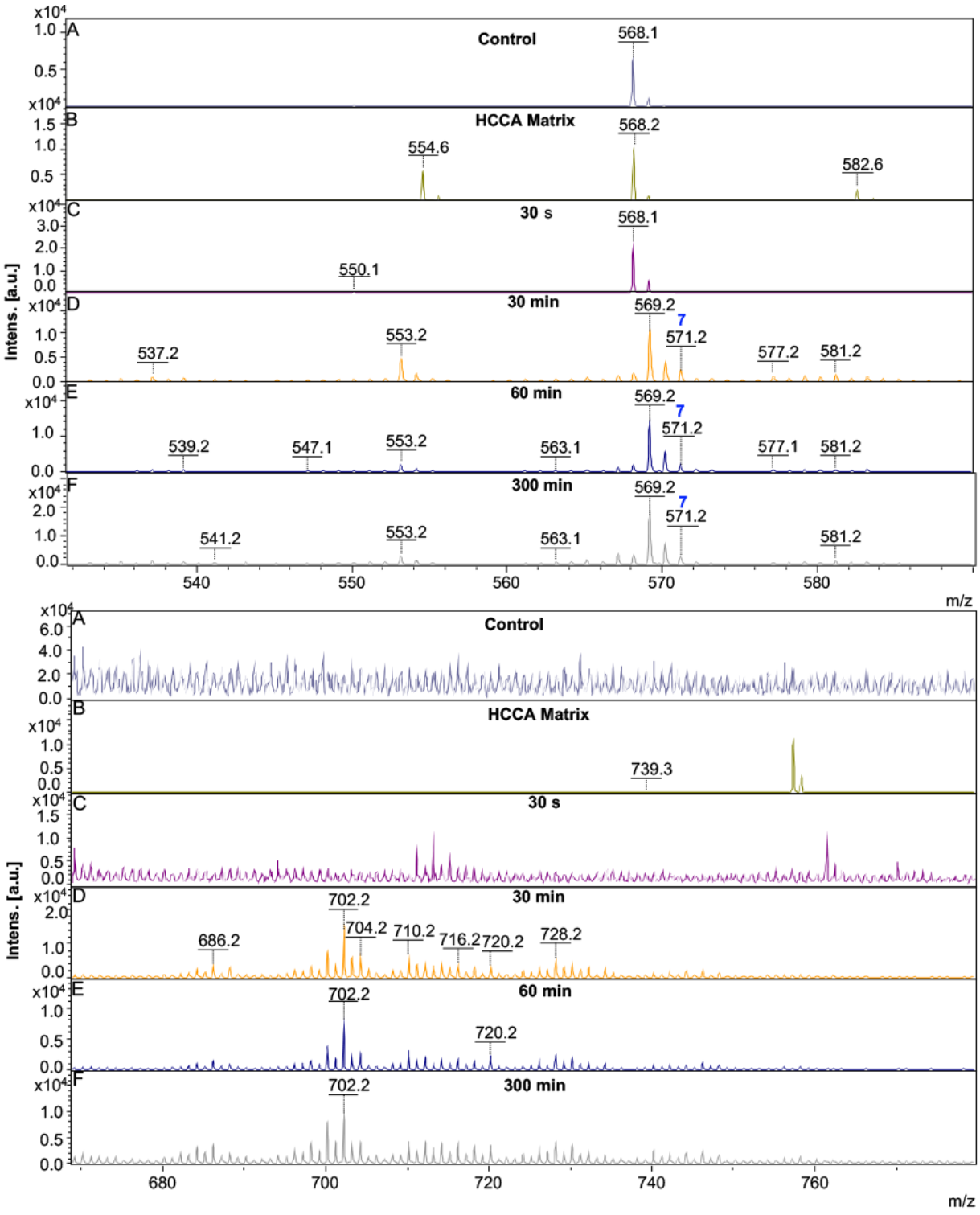

Figure 3.6 (continued) MALDI-TOF mass spectra of PDA formed during the time-course study: A) Control (aqueous dopamine HCl acidified with acetic acid); B) α-cyano-4-hydroxycinnamic acid (HCCA) matrix; C) 30 s; D) 30 mins; E) 60 mins; F) 300 mins.

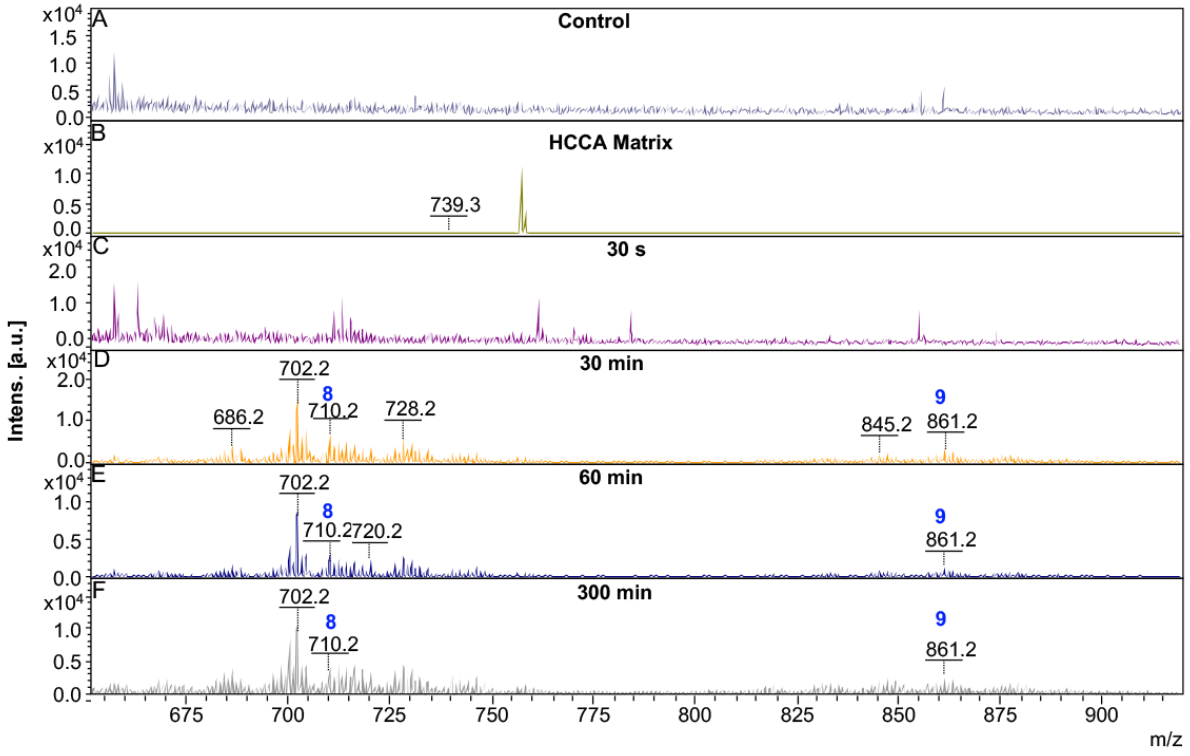

Figure 3.6 (continued) MALDI-TOF mass spectra of PDA formed during the time-course study: A) Control (aqueous dopamine HCl acidified with acetic acid); B) α-cyano-4-hydroxycinnamic acid (HCCA) matrix; C) 30 s; D) 30 mins; E) 60 mins; F) 300 mins.

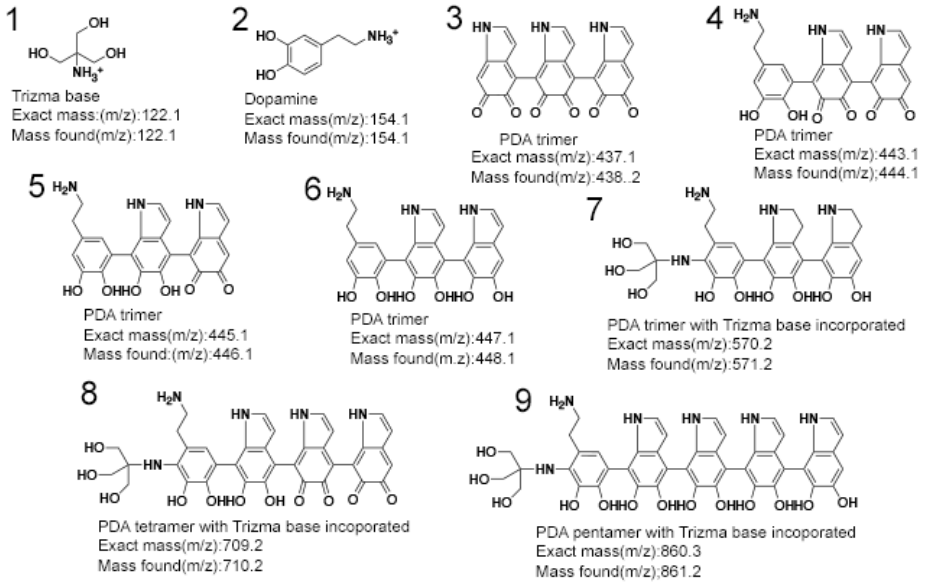

Figure 3.7 Proposed structures associated with peaks are identified in Figure 3.6.

3.2 PDA Degradation

The degradation of PDA is of interest to better understand the stability of PDA coating in different applications.[19] Previous studies[36] indicate that hydrogen peroxide dissociates into hydroxyl radicals in the presence of high alkaline concentration. These hydroxyl ions react with PDA and facilitate its degradation by lessening the π-π interactions that exist between the repeating units of PDA to form fluorescent polydopamine dots.[36] Aside alkalinity of the solution, the degradation process is sped up by heating the reaction.[36] However, in this study, the synthesized PDA was subjected to hydrogen peroxide degradation in the absence of an alkaline medium and at room temperature. This was done to sequentially track the degradation process. Hence, a well-structured degradation study was carried out on the synthesized PDA using 50% hydrogen peroxide. A preliminary degradation study was conducted by varying the concentration of hydrogen peroxide used. The concentrations employed include 1, 2.5, 3.9, 5.4, and 9.8 M. The degradation using these different concentrations produced distinct colors. The higher the concentration of hydrogen peroxide used, the lower the intensity of the brown color observed. Mass spectrometry analysis of the data showed that the higher the concentration of the hydrogen peroxide used, the fewer the peaks that were generated indicates faster degradation of the PDA in that medium.

To study the degradation kinetics, concentrated hydrogen peroxide (50%) was chosen and added to freeze-dried PDA to form a concentration of 10 mg/mL. This sample was monitored over days for a color change. The color change observed was from black color (Figure 3.8A) to deep brown color within 2 days (Figure 3.8B). The deep brown color became lighter within 4 days (Figure 3.8C) and the intensity of the brown color decreased by 8 days (Figure 3.8D). By the 30^{th} day, the color of the reaction solution had changed to yellow (Figure 3.8E) and the

yellow color was maintained even after 60 days (Figure 3.8F). Research indicates that the use of dialysis together with 10% ethanol (ethanol used to quench the hydroxyl radicals produced in the reaction mixture) can be used to purify the degraded products[36]. Nonetheless, in this study, freeze-drying the sample was used to get rid of the hydrogen peroxide in the sample before characterization. The samples corresponding to color changes obtained on the different days (2, 4, 8, and 30) were subjected to UV-Vis and TEM and to prove that hydrogen peroxide mediates the degradation of PDA. NMR and mass spectrometry analysis were carried out to determine the structures obtained from the degradation studies.

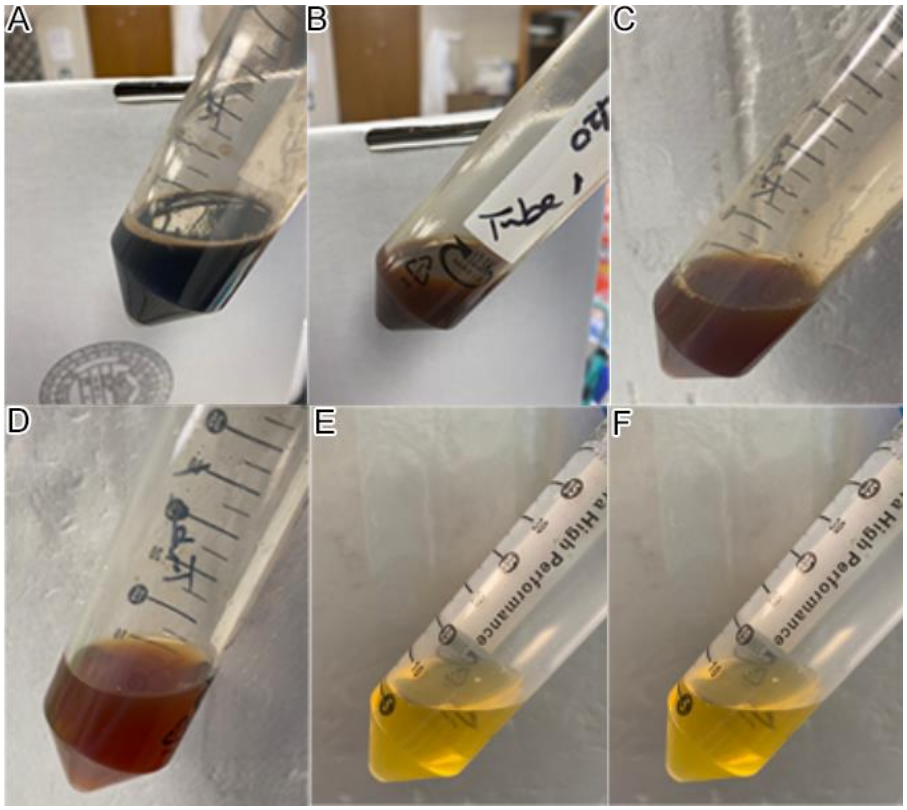

Figure 3.8 Photographs of the color changes of PDA as observed in 50% H_2O_2 associated with synthesized PDA at different incubation times: (A) day 0; (B) day 2; (C) day 4; (D) day 8; (E) day 30; and (F) day 60.

PDA degradation studies of the samples obtained for the different days described in the previous paragraph were monitored using the UV-Vis. The products formed during the degradation period exhibited UV-Vis spectra with no absorbance in the visible region (Figure 3.9A-D). Also, as the days proceeded, there was a gradual decrease in the broad peak formed between 280 nm and 300 nm as identified in the synthesized PDA (Figure 3.2B). This suggests that there was a gradual decrease in the uncyclized dopamine HCl and DHI identified units in the synthesized PDA after degradation. After 30 days of degradation, the broad peak found between 280 nm and 300 nm was no more visible. Previous studies reveal that the disappearance of the broad peak suggests that the proportions of the uncyclized dopamine HCl and DHI units in the 30-day sample might be significantly low. This characteristic of the 30-day resembles that of eumelanin.[19, 36]

The changes in shape and size of the degraded samples were visualized using TEM. The image corresponding to 2-day degraded PDA sample (Figure 3.10B) compared to the image of synthesized PDA sample (Figure 3.10A) revealed some morphological change in the PDA due to the presence of hydrogen peroxide in the reaction mixture. The structural change showed that the particles were interconnected making it difficult to identify individual particles. Previous studies suggest that this kind of interaction might be due to the degradation of catechol groups present in the PDA.[37] This kind of linkage between the particles was also found in the 4-day (Figure 3.10C) and 8-day (Figure 3.10D) degraded samples as well. Prolonging the degradation to 30 days revealed that the interconnection between the particles was broken to form individual particles (Figure 3.10E). In the 30-day degraded sample, both small and large particles were observed with irregular shapes. However, after about 60 days, only small particle sizes were observed with a more defined shape (Figure 3.10F). Also, one significant physical observation that was made is

that; synthesized PDA after freeze-drying had poor solubility in all solvents including water. Nevertheless, the products obtained from the degradation had better solubility in water than the synthesized PDA with the after 30 days degraded sample having the best solubility.

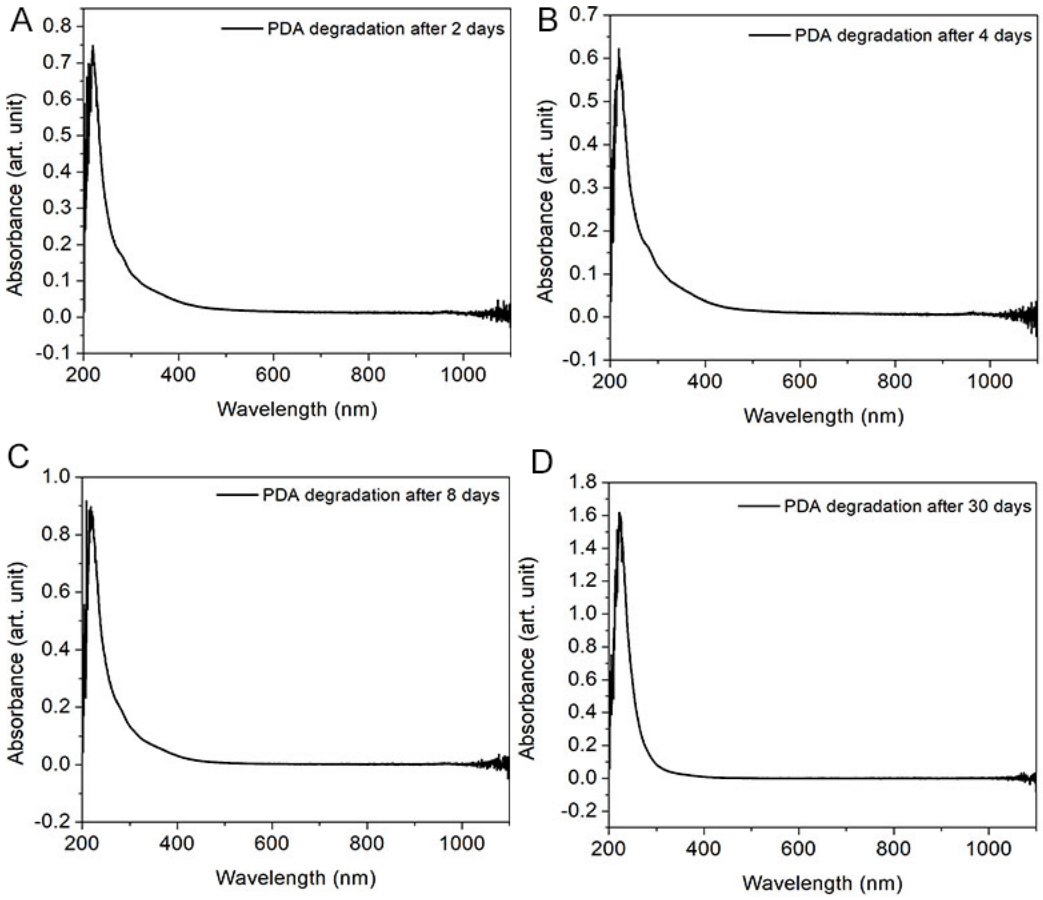

Figure 3.9 UV-Vis spectra of aqueous suspensions of PDA degradation products after different incubation times: (A) day 2; (B) day 4; (C) day 8; and, (D) day 30.

Based on the analysis above, it can be suggested that PDA was formed first by the oxidation of dopamine in the presence of tris buffer and oxygen to form dopaminequinone. This was followed by the intramolecular cyclization of dopaminequinone via 1,4 Michael addition to form leukodopaminechrome. The formed leukodopminechromine underwent oxidation to form

dopaminechrome. This dopaminechrome may undergo intermolecular disproportionation to form 5,6-dihydroxyindole and indole-5,6 quinone units.[18]

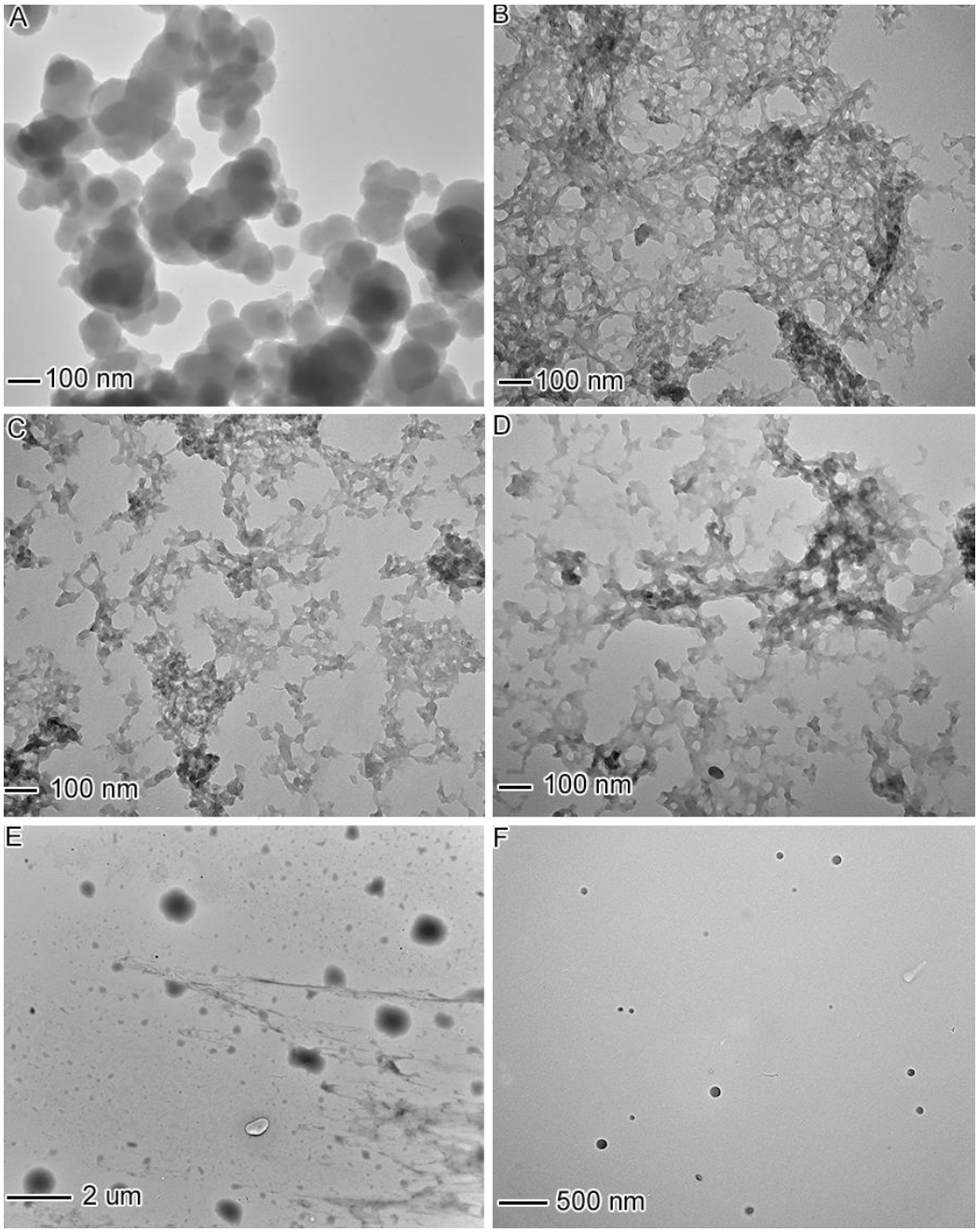

Figure 3.10 TEM images of aliquots taken from PDA degradation products after different incubation time: A) day 0; (B) day 2; (C) day 4; (D) day 8; (E) day 30; and, (F) day 60.

These monomeric units of 5,6-dihydroxyindole and indole-5,6 quinone units covalently combined with uncyclized dopamine HCl that remained unreacted in solution in different ways as illustrated in Figure 3.7 to form oligomers that self-aggregate to form a complex structure of PDA. Then, the degradation of the formed PDA was triggered by the presence of hydrogen peroxide. The hydrogen peroxide split into hydroxyl ions that reacted with the synthesized PDA. The complex structure of the PDA got fragmented into smaller units whose solubility increased with a longer degradation period. The increase in solubility of the PDA degraded products suggests that more hydroxyl groups were being added to the fragmented products.

Further analysis of the degraded samples was carried out using liquid-state ^{1}H NMR in D_2O. The signals of the aromatic protons (H3, H4, and H5) identified as multiplet (6.72-6.89 ppm) in the as-prepared PDA (Figure 3.5B) were also present in degraded products corresponding to after 2 days (Figure 3.11A) and 4 days (Figure 3.11B). Comparing the integrated peaks identified as aromatic protons in the synthesized PDA with those of the after 2 and 4 days, it was observed that, as the degradation proceeded, there was a decrease in the peak area of the degraded products. This result correlated with the results that were observed in the UV-Vis spectra of the degraded samples. Additional analysis of the peak region corresponding to the aromatic protons for after 8 days degraded sample (Figure 3.11C), it was observed that several other peaks were produced making it difficult to differentiate it from the aromatic peaks of interest. Subsequently, from the analysis of the peak region corresponding to the aromatic protons in the after 30 days degraded sample (Figure 3.11D), it was observed that there were no peaks present in the region corresponding to the aromatic protons. This same result was observed in the UV-Vis spectra corresponding to the after 30 days degraded where the broad peak between 280 nm and 300 nm had disappeared. Several other peaks that were absent in the NMR spectrum for the as-prepared

PDA or dopamine HCl were identified in spectra corresponding to the degraded samples (Figure 3.11A-D). These new peaks were found between 1 and 4 ppm. This suggests that the reaction of hydrogen peroxide with the synthesized PDA might have resulted in the breaking down of pi-bonds in the aromatic and pyrrole rings of the repeating units after 30 days of reaction leading to the formation of new structures. To have a better understanding of the structural changes that were observed in the proton NMR spectra of the degraded samples, the degraded samples were subjected to mass spectrometry analysis.

For mass spectrometry analysis of the degraded samples, the samples remained in D_2O. The NMR solvent used was maintained so as not to change the environmental condition of the samples that were being analyzed. The PDA spectrum produced peaks between m/z 300 to m/z 1050 with inconsistency in spacing as opposed to reports of the series of peaks with spacing of m/z 24.[18, 36] The mass spectrometry data revealed that the oligomers that constitute the PDA peaks decreased as the degradation proceeded (Figure 3.12). This result correlated with the decrease in color intensity of the degraded samples formed after the 2-,4-,8- and 30-day degradation periods.-However, in the D_2O environment, the matrix peaks could not be differentiated from peaks associated with PDA oligomers. Also, since D_2O is heavier than water, it was possible to have a shift in peaks for PDA oligomers if they were identified. For better analysis, the PDA degraded samples were, therefore, dissolved in water and subjected to mass spectrometry analysis. In the water medium, the spectra obtained had m/z ranging from 230 to 840 (Figure 3.13). The proposed structures for the peaks labeled with the numbers in blue were identified in Figure 3.14. Peaks labeled with the symbol (*) represent matrix peaks. A peak at m/z 299.1 suggested that PDA degradation yielded a dimer while peaks at m/z 446.2, 450.2, and

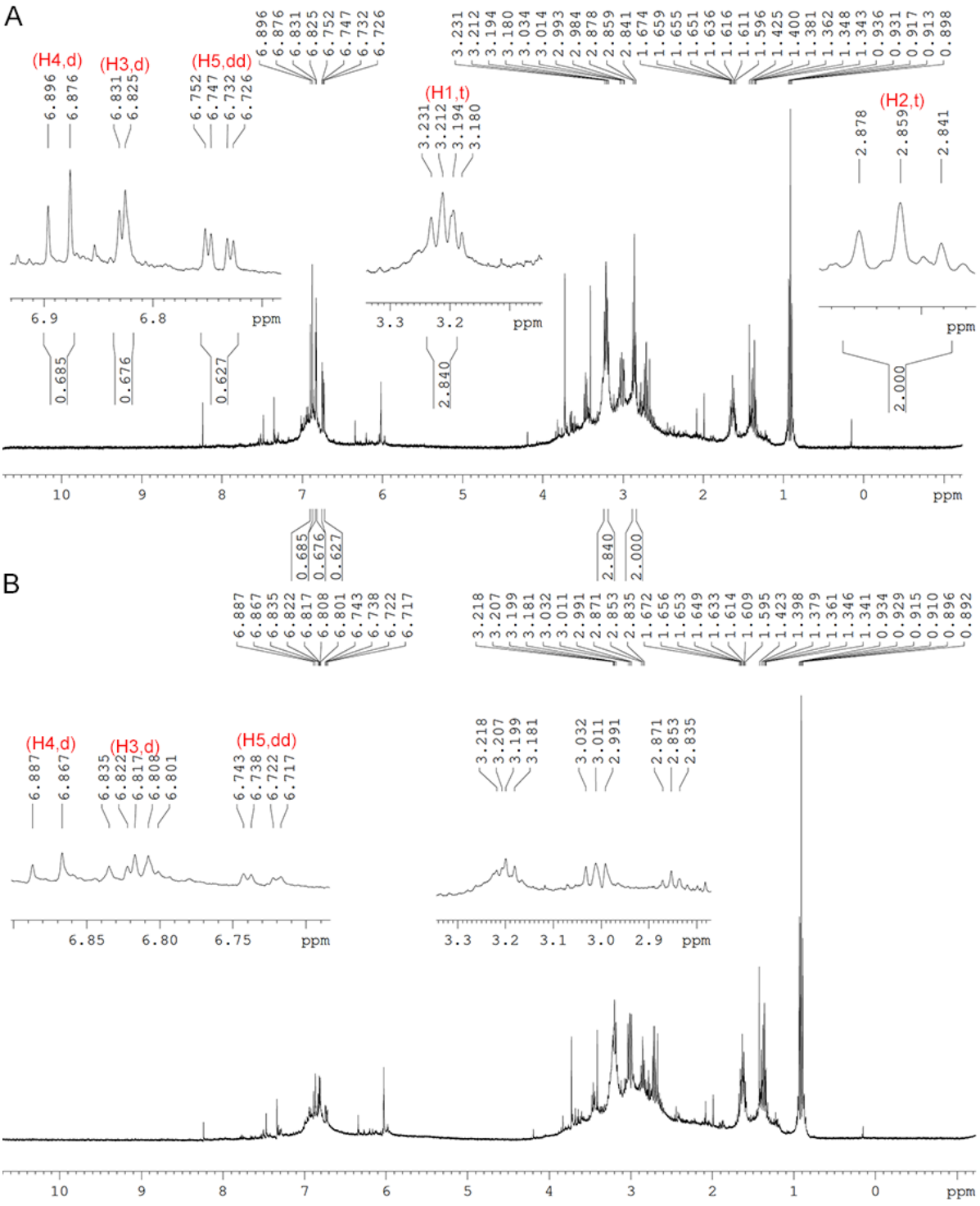

Figure 3.11 ^{1}H NMR spectra of PDA degradation products after different incubation times: (A) day 2;(B) day 4; (C) day 8; and, (D) day 30.

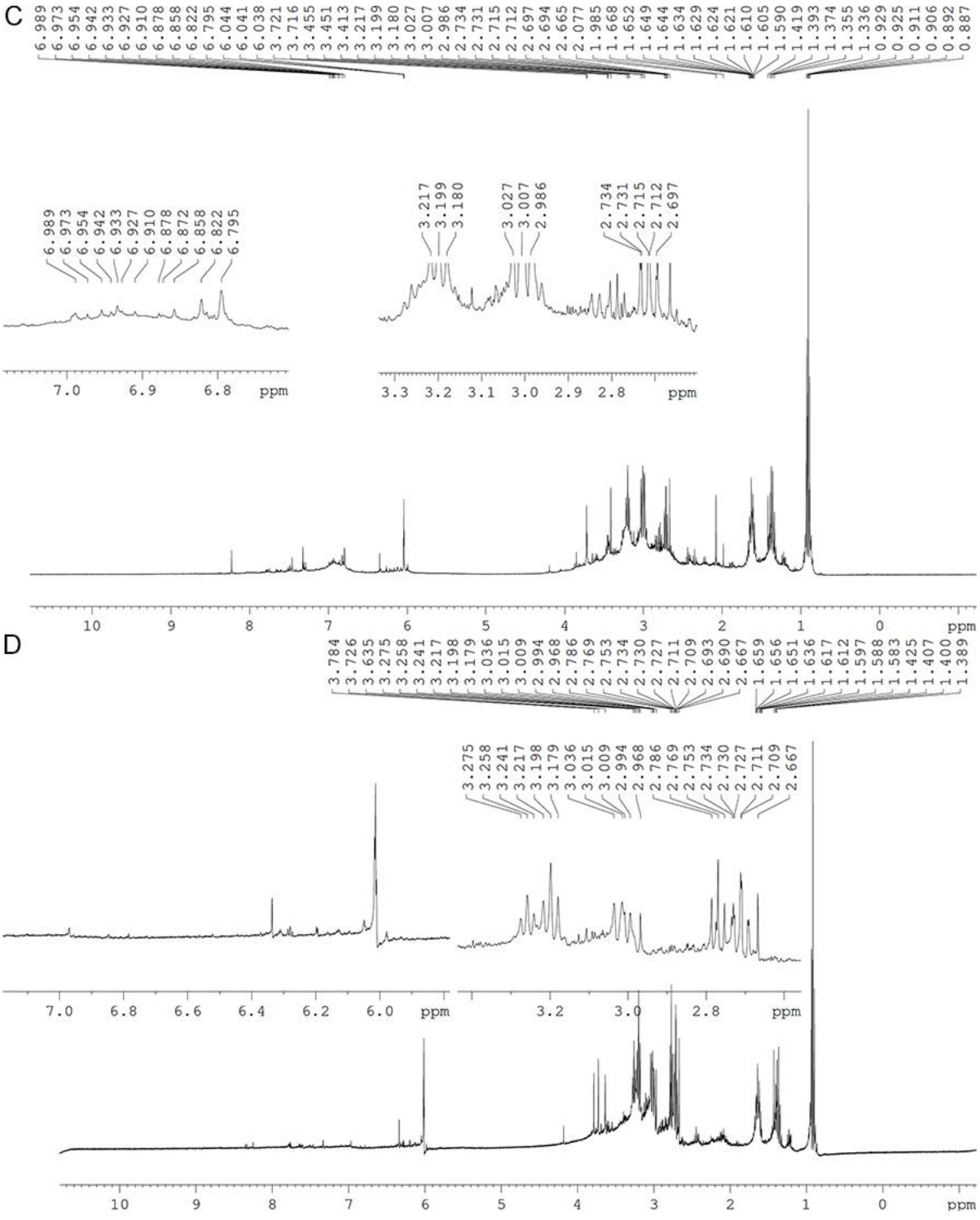

Figure 3.11(continued) ^{1}H NMR spectra of PDA degradation products after different incubation times: (A) day 2;(B) day 4; (C) day 8 and, (D) day 30.

454.1 suggested that PDA degradation yielded PDA trimers. The proposed structures formed indicated that different combination of uncyclized dopamine, DHI and indole-5,6-quinone units covalently bonded together (Figure 3.14). A peak at m/z 299.1 represented two monomers of DHI covalently bonded together, or a monomer of dopamine covalently bonded to a monomer of indole-5,6-quinone. Also, the peak at m/z 446.2 corresponded to a combination of one monomer of dopamine to two monomers of DHI. Subsequently, a peak at 454.1 was associated with two monomers of dopamine covalently bonded to one monomer of DHI.

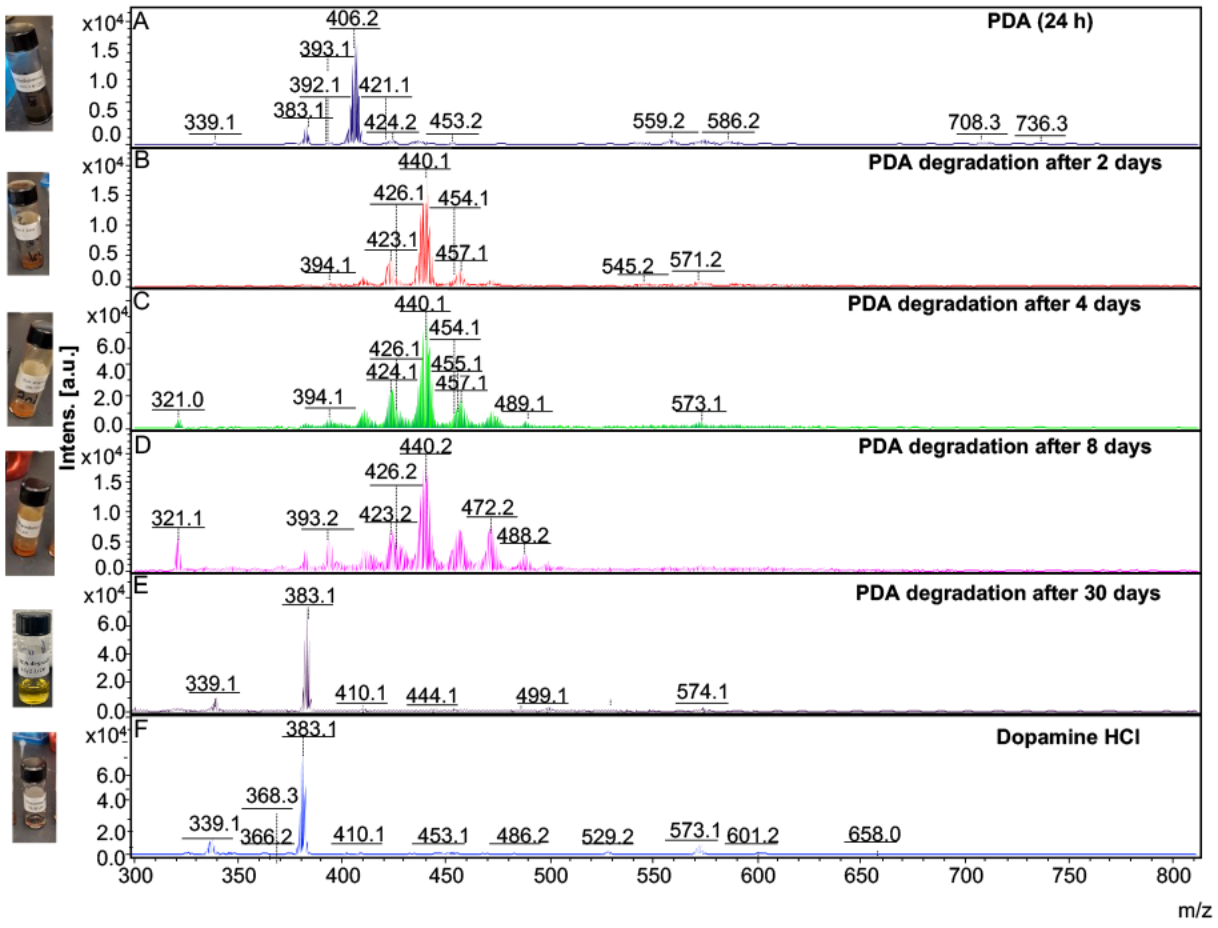

Figure 3.12 MALDI-TOF mass spectra of different samples in D_2O: (A) PDA sample with a reaction time of 24 h; PDA degradation products after different incubation times: (B) day 2; (C) day 4; (D) day 8 and (E)30; (F) Dopamine HCl after few days.

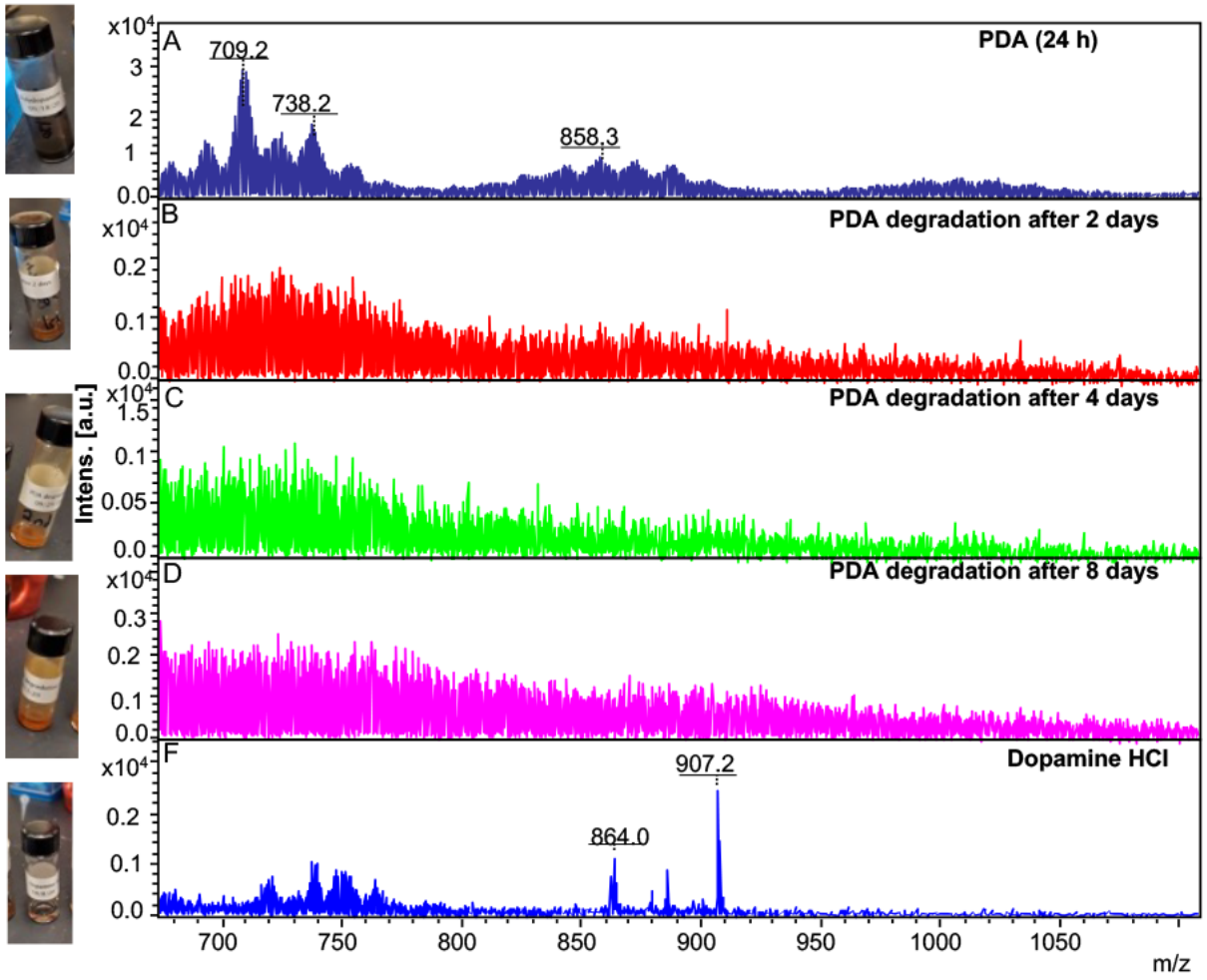

Figure 3.12 (continued) MALDI-TOF mass spectra of different samples in D_2O: (A) PDA sample with a reaction time of 24 h; PDA degradation products after different incubation times: (B) day 2; (C) day 4; (D) day 8 and (E)30; (F) Dopamine HCl after few days.

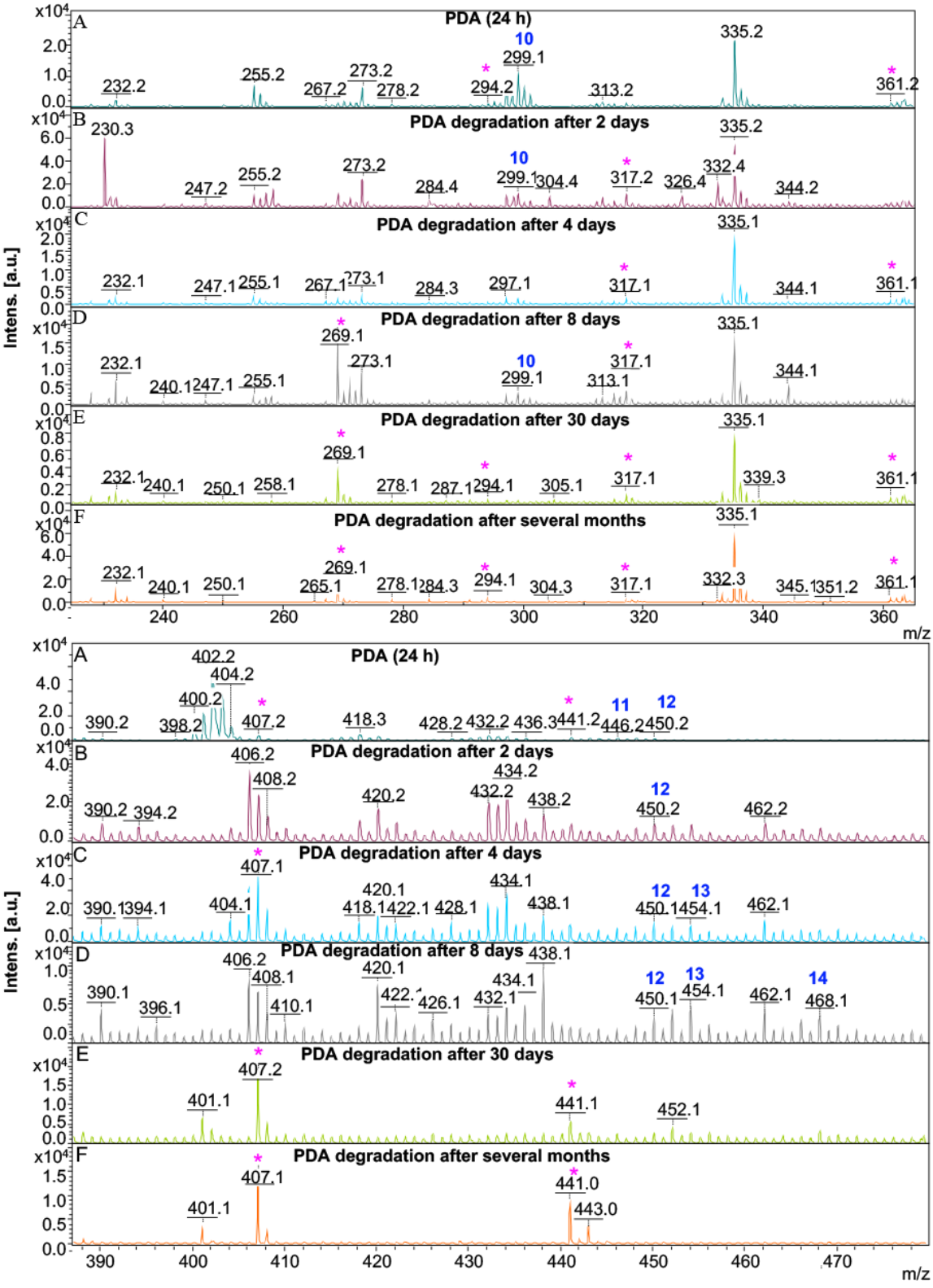

Figure 3.13 MALDI-TOF mass spectra of different samples in H_2O: (A) PDA sample with a reaction time of 24 h; PDA degradation products after different incubation times: (B) day 2; (C) day 4; (D) day 8 and (E) day 30; (F) PDA degradation after several months.

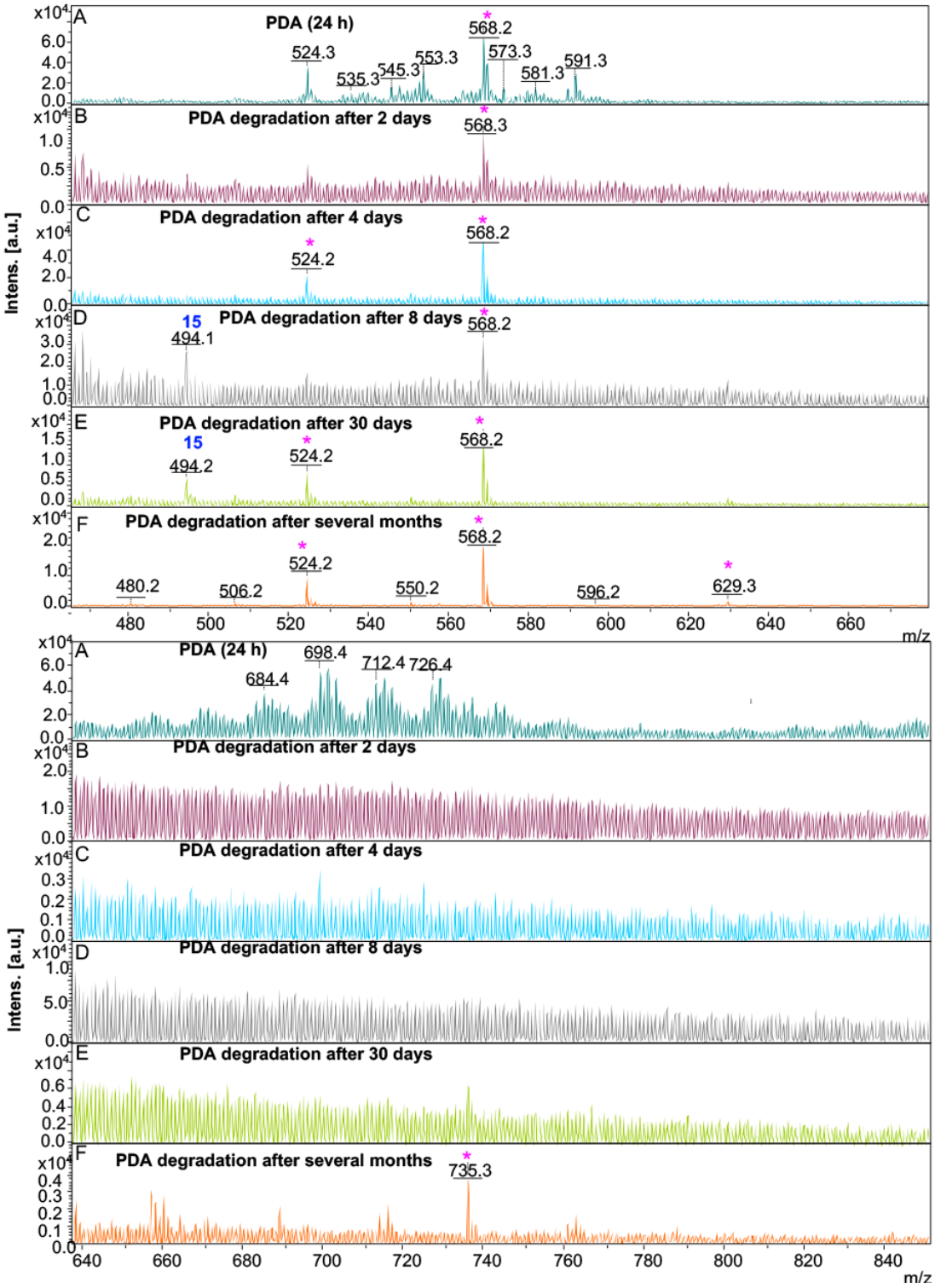

Figure 3.13 (continued) MALDI-TOF mass spectra of different samples in H_2O: (A) PDA sample with a reaction time of 24 h; PDA degradation products after different incubation times: (B) day 2; (C) day 4; (D) day 8 and (E) day 30; (F) PDA degradation after several months.

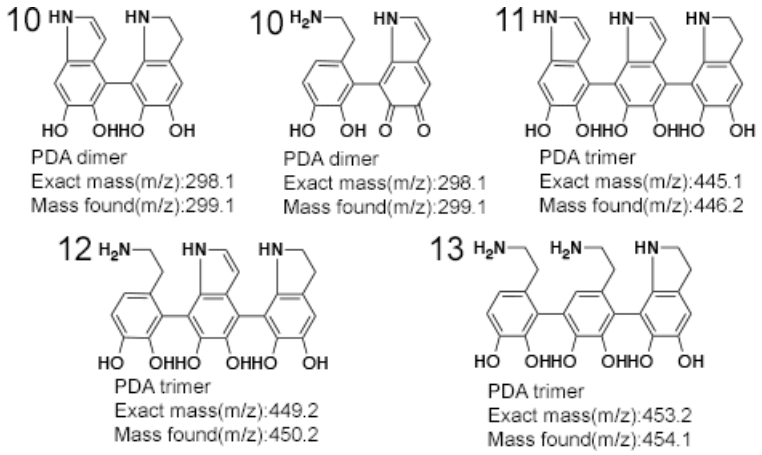

Figure 3.14 Proposed PDA structures associated with PDA peaks identified in MALDI-TOF mass spectra in Figure 3.13.

3.3 Application of PDA Formation

3.3.1 Modification of the Surface of Silica with PDA

PDA coating on various surfaces was made possible because of catechol and amine functional groups present in dopamine.[6] The most common coating process used is the immersion of the material to be coated into dopamine solution which has been buffered at ambient temperature to achieve the PDA coating on the surface of the material of interest.[6] Nevertheless, in this study, a fast deposition method using a dispersion tool that was used for the synthesis of the PDA was adopted to achieve uniform coating thickness on the surface of nanoparticles such as SiO_2. Typically, to prevent the formation of free PDA in solution, the nanoparticle of interest is introduced into the tris base solution before the PDA precursor is added and also to control the proportion of dopamine monomer to a nanoparticle that is being coated. [38] The process leading to the synthesis of SiO_2-PDA core-shell nanoparticles is illustrated in Figure 3.15.

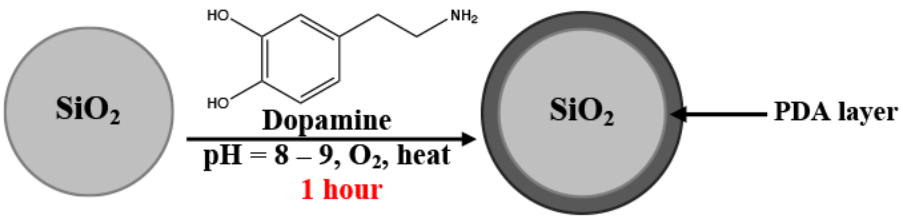

Figure 3.15 Schematic for the formation of SiO_2-PDA core-shell Nanoparticles via deposition of PDA on SiO_2 nanoparticles.

Firstly, the silica nanoparticles were synthesized via the Stöber process. TEOS, ethanol, water, and ammonium hydroxide used in the synthesis of the silica nanoparticles were mixed in a ratio of 1:75:31:4[48]. The silica nanoparticles produced were spherical as shown in the TEM image (Figure 3.16A). These nanoparticles had an average diameter of 376.5 ± 26.3 nm and were well dispersed with no aggregation. After the PDA coating was achieved, there was no change in the average size of the nanoparticles 376.5 ± 31.2 nm. The TEM image of these SiO_2-PDA core-shell nanoparticles (Figure 3.16B) showed that the PDA coating was present but was very thin. Also, not all the silica nanoparticles were covered with the PDA. This indicated that the ratio of the amount of dopamine monomer to the surface area of synthesized silica used was not proportional.

Furthermore, Snowtex ST-PS-M (Nissan Chemical America Corp., Houston, TX), commercial silica which possesses the following properties – particle shape described as a string of pearls and particle size between 18-25 nm – was coated with PDA to be incorporated into PTFE thin films. The essence of the incorporation of SiO_2-PDA into PTFE was to help improve the wear resistance and to reduce friction in the PTFE films. Similar conditions for coating the synthesized SiO_2 with PDA were used. However, in this process, the amount of dopamine HCl used was 44.0 mg due to the small size of the commercial silica. The shape of the commercial silica was described as a string of pearls as illustrated in the TEM image (Figure 3.17A). After

surface functionalization with PDA, the TEM image of the PDA coated commercial SiO_2 (Figure 3.17B) resembled that of the bare silica sample (Figure 3.17A).

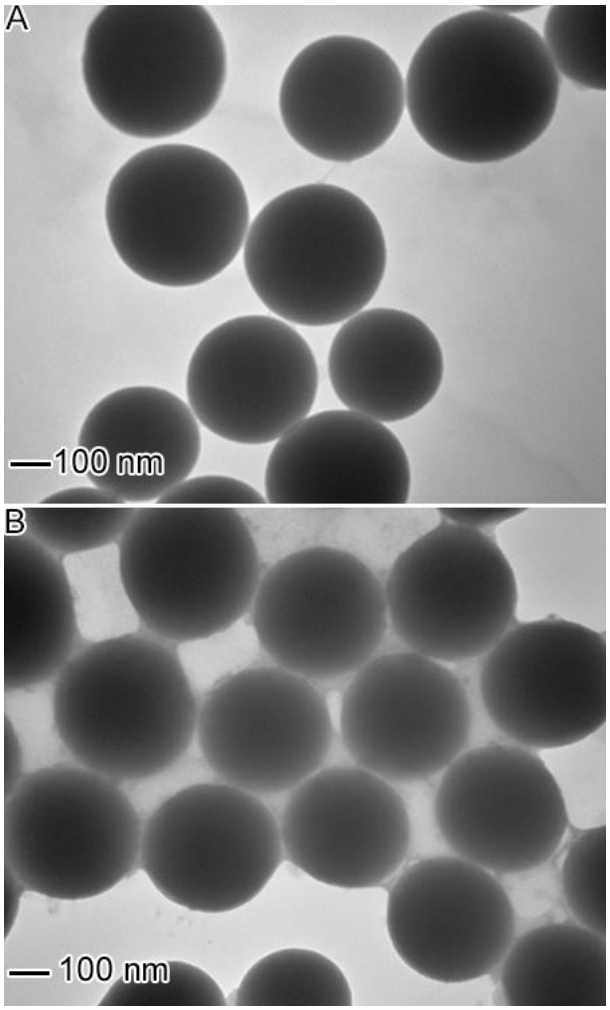

Figure 3.16 TEM images of (A) synthesized bare SiO_2 and, (B) SiO_2-PDA core-shell nanoparticles.

To confirm that the PDA coating was present, the SiO_2-PDA core-shell nanoparticles were etched with varying concentrations of NaOH (1 M and 6 M), to form hollow PDA. However, the use of NaOH as an etchant was not successful. Further characterization using DLS and zeta potential produced a diameter of 106.9 ± 0.7 nm with a zeta potential of -34.51 ± 1.60

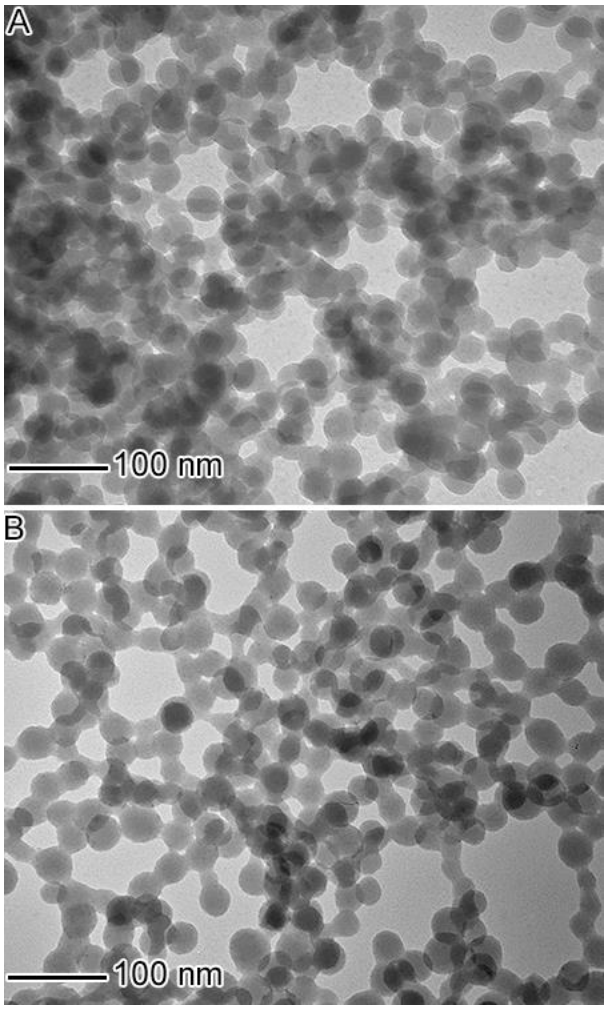

Figure 3.17 TEM images of (A) bare commercial SiO_2 and, (B) commercial SiO_2 coated with PDA to form core-shell nanoparticles.

mV for the bare commercial silica and diameter of 106.8 ± 1.2 nm with a zeta potential of -36.09 ± 1.62 nm for the commercial silica coated with PDA. These results showed no significant difference between the uncoated and coated silica nanoparticles. Hence, to improve upon the coating, the amount of dopamine used was increased by five-fold. The TEM images obtained still did not show any significant difference from images obtained in Figure 3.17B. Hence, to confirm the success of PDA coating, FTIR analysis was used to characterize the bare silica and SiO_2-PDA nanoparticles (Figure 3.18). The peaks identified at 800 cm^{-1} and 1115 cm^{-1}

represented the symmetric and asymmetric vibrations of SiO_2, respectively. Vibrations associated with C=O and C=C functional groups were attributed to peaks at 1706 cm^{-1} and 1631 cm^{-1}, respectively, of the PDA found in SiO_2-PDA core-shell nanoparticles. Also, both SiO_2 and SiO_2-PDA core-shell nanoparticles exhibited peaks at 2928 cm^{-1} and 3447 cm^{-1} corresponding to C-H and O-H vibrations respectively. Yet, the success of the formation of SiO_2-PDA could not be confirmed with this result because of the similarity between the FTIR spectra of SiO_2 and SiO_2-PDA core-shell nanoparticles.

Research indicates that cations such as Cu^{2+} and Fe^{3+} ions can be used as oxidants for the synthesis of PDA.[27] Hence, to improve the PDA coating on the commercial SiO_2, Cu^{2+} ions were introduced in the form of copper sulfate (1.5 mM, 0.075 g) in addition to the use of oxygen as an oxidant. The UV-Vis spectra obtained are illustrated in Figure 3.19. The results showed that the bare silica nanoparticles revealed no absorbance in the ultraviolet and visible regions of the absorption spectrum (Figure 3.19A). This was because silica is optically transparent. However, the PDA showed absorbance in ultraviolet and visible regions of the absorption spectrum with a broad peak between 280 nm and 300 nm indicating the presence of uncyclized dopamine HCl in the synthesized PDA (Figure 3.19C). The absorption spectrum of SiO_2-PDA (Figure 3.19B) obtained was similarly obtained for the synthesized PDA. This result confirmed the success of the coating. Further characterization of the samples was achieved by measuring the hydrodynamic diameter and zeta potentials. The hydrodynamic diameter measurements for SiO_2, SiO_2-PDA, and PDA were 113.2 ± 0.6 nm, 118.4 ± 0.8 nm, and 166 ± 4.0 nm respectively. While measurement of the surface charges recorded were -23.79 ± 2.02 mV, -27.36 ± 2.40 mV and -17.00 ± 2.16 mV for SiO_2, SiO_2-PDA, and PDA respectively. These results as shown in Table 3.3 support the success of the PDA coating on the silica nanoparticles. Hence, by this

experiment, it has been demonstrated that the presence of cations such as Cu^{2+} ions accelerate dopamine oxidation and polymerization to form PDA.

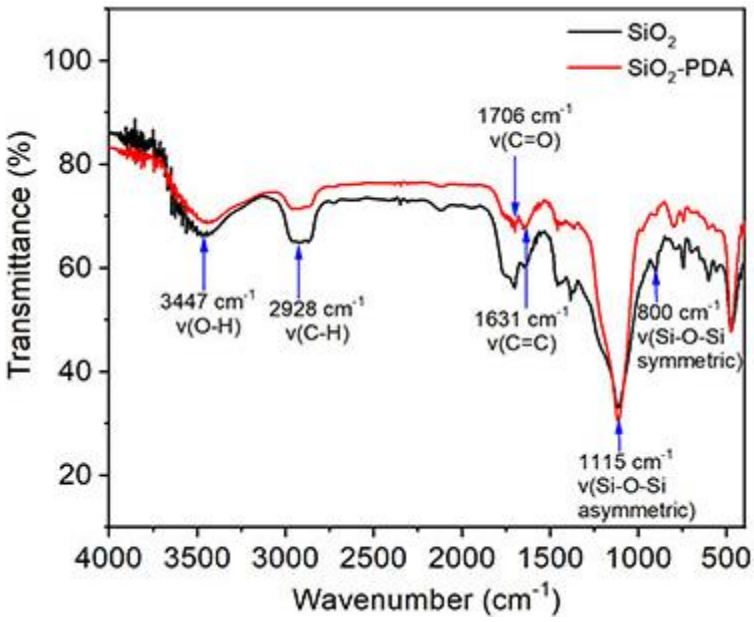

Figure 3.18 IR spectra of commercial SiO_2 and commercial SiO_2 coated with PDA to form core-shell nanoparticles.

Table 3.2 Summary of peak position identified in the IR Spectra shown in Figure 3.18

Functional group	Wavenumber (cm^{-1})
OH	3447
CH	2928
C=O	1706
C=C	1631
Si-O-Si asymmetric	1115
Si-O-Si symmetric	800

3.3.2 Modification of Silica -PDA Core-Shell Nanoparticles with Silver

The adhesive property of PDA was explored and used an intermediate layer for the formation of SiO_2-PDA coated with Ag. The essence of the surface functionalization with PDA was to create a suitable surface for the silver nanoparticles that are formed to bind to. To form SiO_2-PDA coated with Ag, the SiO_2 nanoparticles were synthesized by the Stöber method.[48] The surface of the silica nanoparticles was then functionalized with PDA via the established process previously described in this work. The synthesis of the SiO_2-PDA coated with Ag was achieved via the seed-mediated reaction. The silver precursor, $AgNO_3$, was reduced to form silver nanoparticles on the surface of the SiO_2-PDA using $NaBH_4$ as the reduction agent. The amine and hydroxyl functional groups on the PDA coating on the silica nanoparticles were negatively charged to coordinate with the Ag^+ ions that bound to these negatively charged surfaces and stabilizes them on the surface of the SiO_2-PDA. The Ag nanoparticles formed as seeds with nucleation sites for the formation of silver overlayer on the silica nanoparticles with sodium citrate being used as the reducing agent for the $AgNO_3$. The sodium citrate used in the second step is weaker reducing agent compared to $NaBH_4$. This, therefore, was to allow for further growth of the silver only on the nucleation site already created.[49] The UV-Vis spectrum of the final product formed produced a broad peak at 377 nm (Figure 3.20A). Silica nanoparticles do not reveal absorbance in the UV-Vis spectrum, therefore, absorbance at 377 nm was due to the formation of silver nanoparticles in the reaction mixture. The formed SiO_2-PDA coated with Ag nanoparticles were further characterized using TEM. The TEM image (Figure 3.20B) obtained revealed that only a few SiO_2-PDA nanoparticles were coated with silver nanoparticles, but these did not form core-shells as desired. The silver nanoparticles just got deposited forming a close pack on the entire surface. Also, some of the silver nanoparticles got deposited in solution. This

result revealed that a more controlled addition of the Ag^{+} ions would result in the formation of SiO_2-PDA coated with Ag desired.

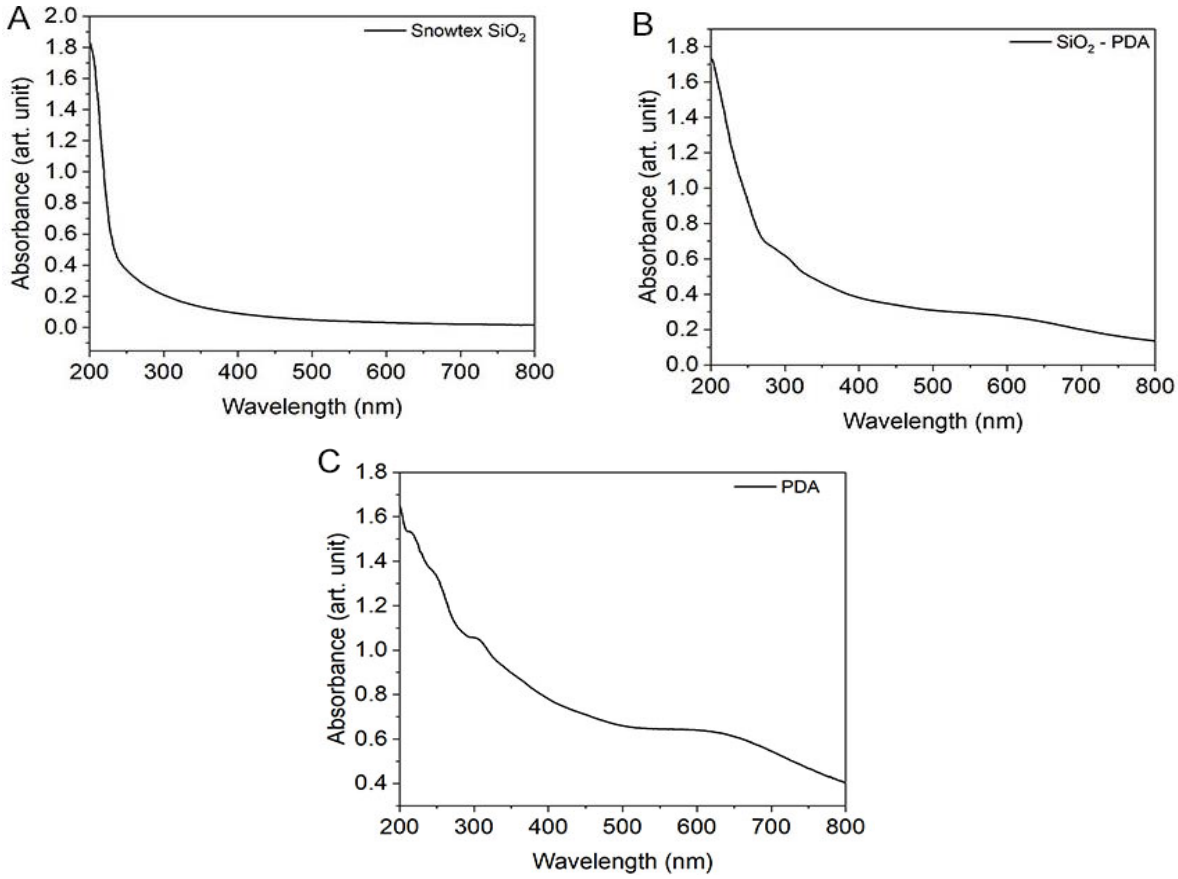

Figure 3.19. UV-Vis spectra showing the spectral changes observed in aqueous suspensions of different samples: (A) commercial SiO_2; (B) commercial SiO_2 coated with PDA; and (C) synthesized PDA.

Table 3.3. Summary of DLS and zeta potential measurements of aqueous suspension different samples.

Sample	Hydrodynamic diameter (nm)	Zeta potential (mV)
SiO_2	113.2 ± 0.6	-23.8 ± 2.1
SiO_2-PDA core-shell	118.4 ± 0.8	-27.4 ± 2.4
PDA	166.1± 4.0	-17.0 ± 2.2

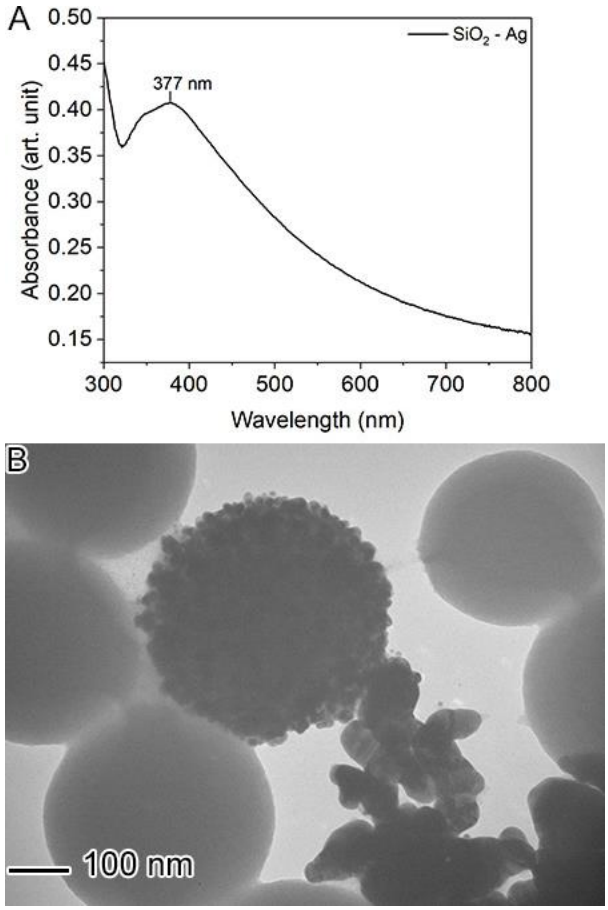

Figure 3.20 Seed-mediated method using $NaBH_4$ and sodium citrate: (A) UV-Vis spectrum of an aqueous suspension of SiO_2-PDA core-shell nanoparticles coated with Ag; (B) TEM images of aqueous suspensions of SiO_2-PDA Core-Shell Nanoparticles coated with Ag.

Hence, to form SiO_2-PDA coated with Ag with a more controlled addition of Ag^+ ions, the reaction was repeated but no seed-mediated method was used. Also, sodium citrate was the only reducing agent used in the reaction. The $AgNO_3$ was added at a slow rate of 0.2 mL/min. With the slow addition of the $AgNO_3$, the color of the reaction mixture gradually changed from the black color associated with the SiO_2-PDA core-shell nanoparticles to an off-white color colloidal suspension. The resulting product formed was characterized with UV-Vis spectroscopy and TEM. The UV-Vis spectrum (Figure 3.21A) produced a broad peak with absorbance at about 410 nm due to the presence of silver nanoparticles in the solution. The TEM image (Figure

3.21B) depicts that the ratio of the SiO_2-PDA to $AgNO_3$ was not equal. Also, silver nanoparticles were formed in solution but did not lead to the formation of the desired SiO_2-Ag core-shell nanoparticles with a PDA adhesion layer as an intermediate.

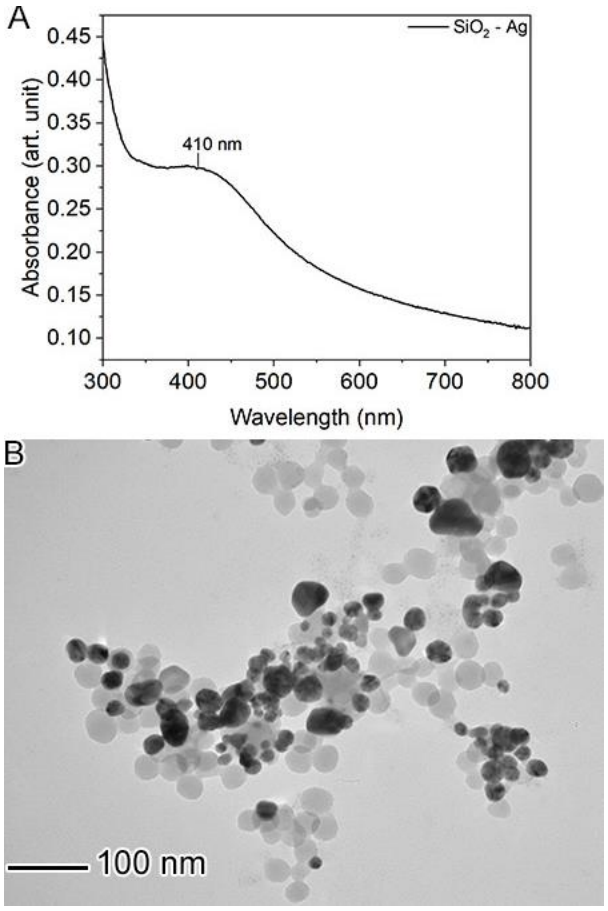

Figure 3.21 (A) UV-Vis spectrum of aqueous suspensions of SiO_2-PDA core-shell nanoparticles coated with Ag. (B) TEM image of aqueous suspensions of SiO_2-PDA core-shell nanoparticles coated with Ag. Sodium citrate was used as a reducing agent.

Research indicates that because sodium is a weaker reducing agent, no reduction of Ag^+ ions usually takes place at temperatures below 75 °C.[49] Hence, the use of both $NaBH_4$ and sodium citrate as reducing agents was used again with the $NaBH_4$ being added in a dropwise manner. The characterization of the product formed produced a UV-Vis spectrum with a peak at

401 nm due to the presence of silver nanoparticles (Figure 3.22A). The TEM image revealed some of SiO_2-PDA core-shell nanoparticles coated with silver nanoparticles (Figure 3.22B).

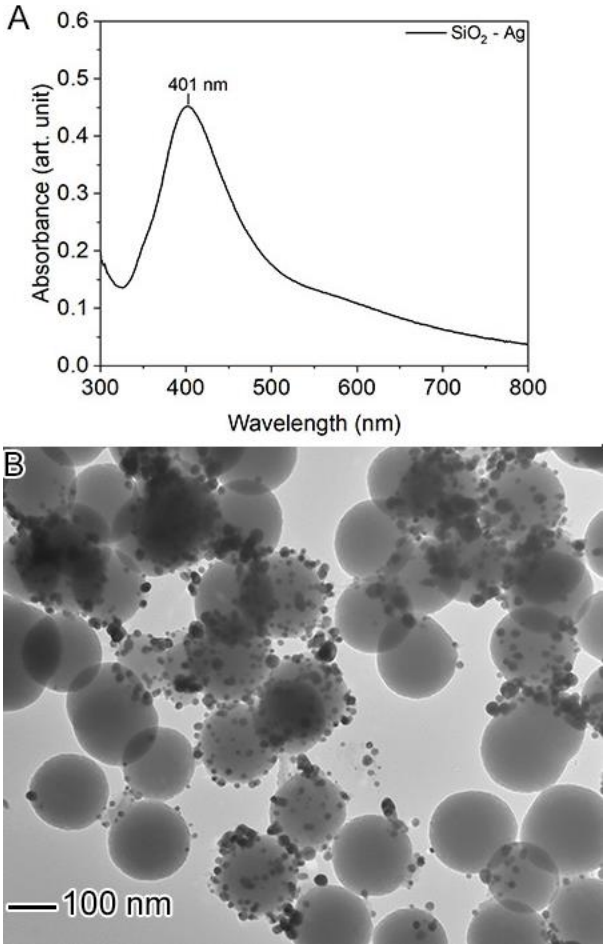

Figure 3.22 (A) UV-Vis spectrum of aqueous suspensions of SiO_2-PDA core-shell nanoparticles coated with Ag. (B) TEM image of aqueous suspensions of SiO_2-PDA core-shell nanoparticles coated with Ag. $NaBH_4$ and sodium citrate were used as reducing agents.

This level of success indicates that surface functionalization of the surface of the silica is critical for success with coating with other nanoparticles such as silver as used in this study. Also, the reducing agent used for the reduction of silver ions is very critical for the formation of nucleation sites on the surface of the silica nanoparticles that will coordinate the formation of silver nanoparticles leading to the formation of the SiO_2-Ag core-shell nanoparticles. This will

prevent the formation of silver nanoparticles in the solution. Finally, the reaction temperature is also important for the formation of SiO_2-Ag core-shell nanoparticles and this is dependent on the reducing agent used. Hence, from this study, the use of both sodium citrate and sodium borohydride as reducing agents at room temperature produced results close to the desired product.

3.3.3 Modification of Surface of PDA with Silver

Due to the low success of the bounded silver nanoparticles to SiO_2-PDA, further study was carried out to investigate the binding of silver nanoparticles to PDA only. The PDA used for this study was synthesized in the presence of oxygen, tris buffer and at a temperature of 50 °C. The dispersion method previously described in this work was used to achieve uniform nanospheres. To obtain the PDA-Ag core-shell nanoparticles, Luo et al. (2015) reported that this can be achieved in the absence of a reducing agent. In their work, they reported that the OH functional group of the PDA can directly reduce Ag^+ ions to form Ag nanoparticles that bind tightly to the surface of the nanoparticles. The particle size of the silver nanoparticles achieved in their work was between 12-18 nm.[50] However, in this work, the desired size of the silver nanoparticles of interest was about 5-10 nm. Hence, to achieve that, different reducing agents together with different reaction conditions were exploited to determine the best reaction condition for the formation of PDA-Ag core-shell nanoparticles. In the first type of reaction, both sodium citrate and sodium borohydride were used as reducing agents for the formation of the silver nanoparticles. The silver ions were first added at a slow rate of 0.2 mL/min to the PDA solution to form uniformly dispersed Ag^+ ions adhered to the PDA. The stabilization of the Ag^+ ions to the binding surface of the PDA was achieved by the addition of sodium citrate which was

acting as a weak reducing agent. The reduction of Ag^+ ions to form Ag nanoparticles bound to the surface of the PDA was achieved by the addition of sodium borohydride at a slow rate of 0.2 mL/min. The TEM image (Figure 3.23) depicts PDA with Ag coating. However, the sizes of the silver nanoparticles were slightly larger than desired and were not of uniform size. The desired size of the silver nanoparticles as the coating was 5 -10 nm.

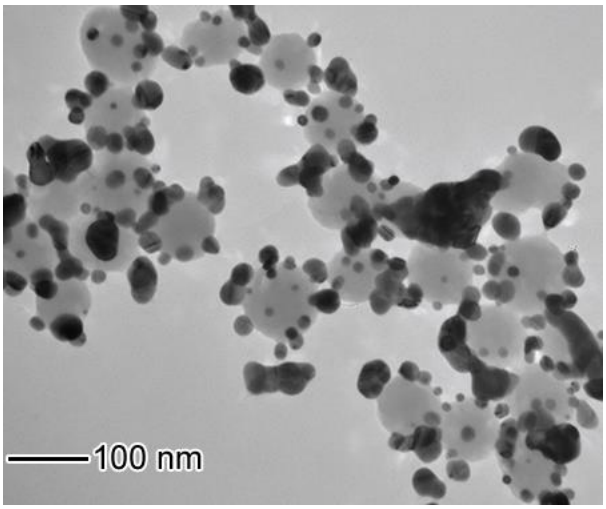

Figure 3.23. TEM image of aqueous suspensions of PDA-Ag core-shell nanoparticles.

Similar to the synthesis of SiO_2-Ag core-shell, the use of only sodium borohydride as a reducing agent produced images of PDA nanoparticles with silver nanoparticles deposited on their surfaces. Yet, the size and shape of these nanoparticles were not uniform and larger than desired. The use of sodium citrate only yielded little to no silver coating on the surface of the nanoparticles. This confirms the report that the reducing capacity of sodium citrate is influenced by temperature. Similar results were obtained when ascorbic acid was used as a reducing agent for the silver nanoparticles. Sodium ascorbate used as a reducing agent at the same concentration (5 mM) used for ascorbic acid produced more silver in solution than when ascorbic acid was used. However, the silver nanoparticles were formed in solution and did not coat the PDA

nanoparticles as desired. These results suggest that the use of both sodium citrate and sodium borohydride is important in controlling the size and shape of the silver nanoparticles coating the surface of the PDA nanoparticles. Hence, further study will be carried out by varying the concentrations of these reducing agents used until the desired size of the silver nanoparticles are achieved.

4 Conclusion and Future Work

An established dispersion method was used for the synthesis of PDA which took place at room temperature for 24 h. PDA was successfully synthesized using 0.6 g of dopamine HCl in 200 mL of water containing 0.242 g of Trizma base. The as-synthesized PDA was characterized to study the chemical structures leading to the formation of PDA. Analysis of the as-synthesized PDA using spectroscopic tools such as mass spectrometry, NMR, and FTIR revealed that PDA structures were covalently bonded together to form a different degree of oligomers. The oligomers were made up of repeated units of dopamine, 5,6-diydroxyindole, and indole-5,6-quinone. The concentration and molar mass of these oligomers increased with the time of formation. The as-synthesized PDA was not completely soluble in water or any other solvent. However, studying the stability of PDA by dissolving the as-synthesized PDA in H_2O_2 to form a solution with a concentration of 10 mg/mL produced PDA structures that were more water-soluble. The analysis of these degraded products with the same spectroscopic tools used to characterize the as-synthesized PDA revealed that the repeated units of PDA remained unchanged and usually formed dimer and trimer units of the PDA structures.

Application of formed PDA as coating material leading to the formation of SiO_2-PDA core-shell nanoparticles revealed that oxidants such as Cu^{2+} could be used together with oxygen to achieve PDA coating on the surface of SiO_2 nanoparticles. Also, in the synthesis of SiO_2-Ag core-shell nanoparticles, the adhesive property of PDA could be employed as an adhesive and intermediate layer between SiO_2 and Ag. However, the success of the formation SiO_2-Ag was also dependent on the kind of reducing agent used. In this research conducted, the use of both sodium citrate and sodium borohydride as reducing agents proved to be the best for achieving SiO_2-Ag formation. However, the ratio of SiO_2 to Ag needs to be fine-tuned to achieve uniform

Ag deposition on SiO_2. Similar to the SiO_2-Ag formation, the synthesis of PDA-Ag nanoparticles can be achieved using both sodium citrate and sodium borohydride as reducing agents to control the size and shape of the Ag coating on PDA nanoparticles surfaces. The future work is to study the formation and stability of PDA structures under different conditions such as various pH and buffer solutions. In addition, further studies are needed to improve upon the synthesis of SiO_2-PDA, SiO_2-Ag, and PDA-Ag core-shell to achieve uniform core-shell formation.

References

1. Chen, C. T.; Chuang , C.; Cao, J. S.; Ball, V.; Ruch, D.; Buehler, M. J., Excitonic Effects from Geometric Order and Disorder Explain Broadband Optical Absorption in Eumelanin. *Nature Communications* **2014,** *5, 3859.*

2. Alfieri, M. L.; Micillo, R.; Panzella, L.; Crescenzi, O.; Oscurato, S. L.; Maddalena, P.; Napolitano, A.; Ball, V.; d'Ischia, M., Structural Basis of Polydopamine Film Formation: Probing 5,6-Dihydroxyindole-Based Eumelanin Type Units and the Porphyrin Issue. *Acs Applied Materials & Interfaces* **2018,** *10* (9), 7670-7680.

3. Lee, H.; Scherer, N. F.; Messersmith, P. B., Single-Molecule Mechanics of Mussel Adhesion. *Proceedings of the National Academy of Sciences of the United States of America* **2006,** *103* (35), 12999-13003.

4. Yu, J.; Wei, W.; Danner, E.; Ashley, R. K.; Israelachvili, J. N.; Waite, J. H., Mussel Protein Adhesion Depends on Interprotein Thiol-Mediated Redox Modulation. *Nature Chemical Biology* **2011,** *7* (9), 588-590.

5. Lim, C.; Huang, J.; Kim, S.; Lee, H.; Zeng, H.; Hwang, D. S., Nanomechanics of Poly(catecholamine) Coatings in Aqueous Solutions. *Angewandte Chemie-International Edition* **2016,** *55* (10), 3342-3346.

6. Lee, H.; Dellatore, S. M.; Miller, W. M.; Messersmith, P. B., Mussel-inspired Surface Chemistry for Multifunctional Coatings. *Science* **2007,** *318* (5849), 426-430.

7. d'Ischia, M.; Napolitano, A.; Ball, V.; Chen, C. T.; Buehler, M. J., Polydopamine and Eumelanin: From Structure-Property Relationships to a Unified Tailoring Strategy. *Accounts of Chemical Research* **2014,** *47* (12), 3541-3550.

8. Lyu, Q. H.; Hsueh, N.; Chai, C. L. L., Direct Evidence for the Critical Role of 5,6-Dihydroxyindole in Polydopamine Deposition and Aggregation. *Langmuir* **2019,** *35* (15), 5191-5201.

9. Liu, Y. L.; Ai, K. L.; Lu, L. H., Polydopamine and Its Derivative Materials: Synthesis and Promising Applications in Energy, Environmental, and Biomedical Fields. *Chemical Reviews* **2014,** *114* (9), 5057-5115.

10. d'Ischia, M.; Napolitano, A.; Pezzella, A.; Meredith, P.; Sarna, T., Chemical and Structural Diversity in Eumelanins: Unexplored Bio-Optoelectronic Materials. *Angewandte Chemie-International Edition* **2009,** *48* (22), 3914-3921.

11. Meredith, P.; Bettinger, C. J.; Irimia-Vladu, M.; Mostert, A. B.; Schwenn, P. E., Electronic and Optoelectronic Materials and Devices Inspired by Nature. *Reports on Progress in Physics* **2013,** *76* (3), 34501.

12. Shanmuganathan, K.; Cho, J. H.; Iyer, P.; Baranowitz, S.; Ellison, C. J., Thermooxidative Stabilization of Polymers Using Natural and Synthetic Melanins. *Macromolecules* **2011,** *44* (24), 9499-9507.

13. Chen, X.; Yan, Y.; Mullner, M.; van Koeverden, M. P.; Noi, K. F.; Zhu, W.; Caruso, F., Engineering Fluorescent Poly(dopamine) Capsules. *Langmuir* **2014,** *30* (10), 2921-2925.

14. Cui, J. W.; Yan, Y.; Such, G. K.; Liang, K.; Ochs, C. J.; Postma, A.; Caruso, F., Immobilization and Intracellular Delivery of an Anticancer Drug Using Mussel-inspired Polydopamine Capsules. *Biomacromolecules* **2012,** *13* (8), 2225-2228.

15. Kasemset, S.; Lee, A.; Miller, D. J.; Freeman, B. D.; Sharma, M. M., Effect of Polydopamine Deposition Conditions on Fouling Resistance, Physical Properties, and Permeation Properties of Reverse Osmosis Membranes in Oil/Water Separation. *Journal of Membrane Science* **2013,** *425*, 208-216.

16. Kang, S. M.; Hwang, N. S.; Yeom, J.; Park, S. Y.; Messersmith, P. B.; Choi, I. S.; Langer, R.; Anderson, D. G.; Lee, H., One-Step Multipurpose Surface Functionalization by Adhesive Catecholamine. *Advanced Functional Materials* **2012,** *22* (14), 2949-2955.

17. Circu, M.; Filip, C., Closer to the Polydopamine Structure: New Insights from a Combined C-13/H-1/H-2 Solid-State NMR Study on Deuterated Samples. *Polymer Chemistry* **2018,** *9* (24), 3379-3387.

18. Dreyer, D. R.; Miller, D. J.; Freeman, B. D.; Paul, D. R.; Bielawski, C. W., Elucidating the Structure of Poly(dopamine). *Langmuir* **2012,** *28* (15), 6428-6435.

19. Della Vecchia, N. F.; Avolio, R.; Alfe, M.; Errico, M. E.; Napolitano, A.; d'Ischia, M., Building-Block Diversity in Polydopamine Underpins a Multifunctional Eumelanin-Type Platform Tunable Through a Quinone Control Point. *Advanced Functional Materials* **2013,** *23* (10), 1331-1340.

20. Della Vecchia, N. F.; Luchini, A.; Napolitano, A.; D'Errico, G.; Vitiello, G.; Szekely, N.; d'Ischia, M.; Paduano, L., Tris Buffer Modulates Polydopamine Growth, Aggregation, and Paramagnetic Properties. *Langmuir* **2014,** *30* (32), 9811-9818.

21. Ding, Y. H.; Weng, L. T.; Yang, M.; Yang, Z. L.; Lu, X.; Huang, N.; Leng, Y., Insights into the Aggregation/Deposition and Structure of a Polydopamine Film. *Langmuir* **2014,** *30* (41), 12258-12269.

22. Salomaki, M.; Marttila, L.; Kivela, H.; Ouvinen, T.; Lukkari, J., Effects of pH and Oxidants on the First Steps of Polydopamine Formation: A Thermodynamic Approach. *Journal of Physical Chemistry B* **2018,** *122* (24), 6314-6327.

23. Zheng, W. C.; Fan, H. L.; Wang, L.; Jin, Z. X., Oxidative Self-Polymerization of Dopamine in an Acidic Environment. *Langmuir* **2015,** *31* (42), 11671-11677.

24. Bian, S. W.; Liu, S.; Chang, L., Synthesis of Magnetically Recyclable Fe3O4@Polydopamine-Pt Composites and their Application in Hydrogenation Reactions. *Journal of Materials Science* **2016,** *51* (7), 3643-3649.

25. Xi, J. B.; Xiao, J. W.; Xiao, F.; Jin, Y. X.; Dong, Y.; Jing, F.; Wang, S., Mussel-inspired Functionalization of Cotton for Nano-catalyst Support and Its Application in a Fixed-bed System with High Performance. *Scientific Reports* **2016,** *6*, 21904.

26. Hu, H. W.; Xin, J. H.; Hu, H., Highly Efficient Graphene-Based Ternary Composite Catalyst with Polydopamine Layer and Copper Nanoparticles. *Chempluschem* **2013,** *78* (12), 1483-1490.

27. Ball, V.; Gracio, J.; Vila, M.; Singh, M. K.; Metz-Boutigue, M. H.; Michel, M.; Bour, J.; Toniazzo, V.; Ruch, D.; Buehler, M. J., Comparison of Synthetic Dopamine-Eumelanin Formed in the Presence of Oxygen and Cu2+ Cations as Oxidants. *Langmuir* **2013,** *29* (41), 12754-12761.

28. Chan, W., Investigation of the Chemical Structure and Formation Mechanism of Polydopamine from Self-Assembly of Dopamine by Liquid Chromatography/Mass Spectrometry Coupled with Isotope-Labelling Techniques. *Rapid Communications in Mass Spectrometry* **2019,** *33* (5), 429-436.

29. Yu, F.; Chen, S. G.; Chen, Y.; Li, H. M.; Yang, L.; Chen, Y. Y.; Yin, Y. S., Experimental and Theoretical Analysis of Polymerization Reaction Process on the Polydopamine Membranes and Its Corrosion Protection Properties for 304 Stainless Steel. *Journal of Molecular Structure* **2010,** *982* (1-3), 152-161.

30. Wang, X. Y.; Jin, B. K.; Lin, X. Q., In-situ FTIR Spectroelectrochemical Study of Dopamine at a Glassy Carbon Electrode in a Neutral Solution. *Analytical Sciences* **2002,** *18* (8), 931-933.

31. Osullivan, D. G., Vibrational Frequency Correlations in Heterocyclic Molecules .7. Spectral Features of a Range of Compounds Possessing a Benzene Ring Fused to a 5-Membered Ring. *Journal of the Chemical Society* **1960,** (Aug), 3278-3284.

32. Xi, Z. Y.; Xu, Y. Y.; Zhu, L. P.; Wang, Y.; Zhu, B. K., A Facile Method of Surface Modification for Hydrophobic Polymer Membranes Based on the Adhesive Behavior of Poly(DOPA) and Poly(dopamine). *Journal of Membrane Science* **2009,** *327* (1-2), 244-253.

33. Liebscher, J.; Mrowczynski, R.; Scheidt, H. A.; Filip, C.; Hadade, N. D.; Turcu, R.; Bende, A.; Beck, S., Structure of Polydopamine: A Never-Ending Story? *Langmuir* **2013,** *29* (33), 10539-10548.

34. Li, B.; Liu, W. P.; Jiang, Z. Y.; Dong, X.; Wang, B. Y.; Zhong, Y. R., Ultrathin and Stable Active Layer of Dense Composite Membrane Enabled by Poly(dopamine). *Langmuir* **2009,** *25* (13), 7368-7374.

35. Hong, S.; Na, Y. S.; Choi, S.; Song, I. T.; Kim, W. Y.; Lee, H., Non-Covalent Self-Assembly and Covalent Polymerization Co-Contribute to Polydopamine Formation. *Advanced Functional Materials* **2012,** *22* (22), 4711-4717.

36. Lin, J. H.; Yu, C. J.; Yang, Y. C.; Tseng, W. L., Formation of Fluorescent Polydopamine Dots from Hydroxyl Radical-induced Degradation of Polydopamine Nanoparticles. *Physical Chemistry Chemical Physics* **2015,** *17* (23), 15124-15130.

37. Chen, X.; Yang, W. D.; Zhang, J. J.; Zhang, L.; Shen, H. Y.; Shi, D. J., Alkalinity Triggered the Degradation of Polydopamine Nanoparticles. *Polymer Bulletin* **2020**, 78(8), 4439.

38. Orishchin, N.; Crane, C. C.; Brownell, M.; Wang, T. J.; Jenkins, S.; Zou, M.; Nair, A.; Chen, J. Y., Rapid Deposition of Uniform Polydopamine Coatings on Nanoparticle Surfaces with Controllable Thickness. *Langmuir* **2017,** *33* (24), 6046-6053.

39. Ju, K. Y.; Lee, Y.; Lee, S.; Park, S. B.; Lee, J. K., Bioinspired Polymerization of Dopamine to Generate Melanin-Like Nanoparticles Having an Excellent Free-Radical-Scavenging Property. *Biomacromolecules* **2011,** *12* (3), 625-632.

40. Tran, M. L.; Powell, B. J.; Meredith, P., Chemical and Structural Disorder in Eumelanins: A Possible Explanation for Broadband Absorbance. *Biophysical Journal* **2006,** *90* (3), 743-752.

41. Yu, X.; Fan, H. L.; Liu, Y.; Shi, Z. J.; Jin, Z. X., Characterization of Carbonized Polydopamine Nanoparticles Suggests Ordered Supramolecular Structure of Polydopamine. *Langmuir* **2014,** *30* (19), 5497-5505.

42. Niyonshuti, II; Krishnamurthi, V. R.; Okyere, D.; Song, L.; Benamara, M.; Tong, X.; Wang, Y.; Chen, J. Y., Polydopamine Surface Coating Synergizes the Antimicrobial Activity of Silver Nanoparticles. *ACS Applied Materials & Interfaces* **2020,** *12* (36), 40067-40077.

43. Okuda, H.; Wakamatsu, K.; Ito, S.; Sota, T., Possible Oxidative Polymerization Mechanism of 5,6-Dihydroxyindole from A Initio Calculations. *Journal of Physical Chemistry A* **2008,** *112* (44), 11213-11222.

44. Mishra, O. P.; Popov, A. V.; Pietrofesa, R. A.; Christofidou-Solomidou, M., Gamma-irradiation Produces Active Chlorine Species (ACS) in Physiological Solutions: Secoisolariciresinol Diglucoside (SDG) Scavenges ACS - A Novel Mechanism of DNA Radioprotection. *Biochimica Et Biophysica Acta-General Subjects* **2016,** *1860* (9), 1884-1897.

45. Demura, M.; Yoshida, T.; Hirokawa, T.; Kumaki, Y.; Aizawa, T.; Nitta, K.; Bitter, I.; Toth, K., Interaction of Dopamine and Acetylcholine with an Amphiphilic Resorcinarene Receptor in Aqueous Micelle System. *Bioorganic & Medicinal Chemistry Letters* **2005,** *15* (5), 1367-1370.

46. Bisaglia, M.; Mammi, S.; Bubacco, L., Kinetic and Structural Analysis of the Early Oxidation Products of Dopamine - Analysis of the Interactions with Alpha-Synuclein. *Journal of Biological Chemistry* **2007,** *282* (21), 15597-15605.

47. Ryu, J. H.; Messersmith, P. B.; Lee, H., Polydopamine Surface Chemistry: A Decade of Discovery. *ACS Applied Materials & Interfaces* **2018,** *10* (9), 7523-7540.

48. Sreedhar, B.; Radhika, P.; Neelima, B.; Hebalkar, N., Synthesis and Characterization of Silica@Copper Core-Shell Nanoparticles: Application for Conjugate Addition Reactions. *Chemistry-an Asian Journal* **2008,** *3* (7), 1163-1169.

49. Jiang, Z. J.; Liu, C. Y., Seed-Mediated Growth Technique for the Preparation of a Silver Nanoshell on a Silica Sphere. *Journal of Physical Chemistry B* **2003,** *107* (45), 12411-12415.

50. Luo, H. Y.; Gu, C. W.; Zheng, W. H.; Dai, F.; Wang, X. L.; Zheng, Z., Facile Synthesis of Novel Size-Controlled Antibacterial Hybrid Spheres using Silver Nanoparticles Loaded with Poly-dopamine Spheres. *RSC Advances* **2015,** *5* (18), 13470-13477.

Appendix A: Description of Research for Popular Publication

Polydopamine(PDA) is a polymer produced by chemical oxidation of dopamine under basic medium. It possesses prominent properties such as having strong adhesive properties, being magnetic, and compatible with biological materials. These properties among others explain the multifunctional ability of PDA and its rapid emergence in fields such as material science, biomedicine, and energy conversion. For example, dopamine is employed in the functionalization the surfaces of many materials ranging from metals to polymers due to the strong adhesive property. The strong adhesive proprtery is due to the presence catechol and amine functional groups as it exist in amino acids such as lysine and 3,4-dihydroxy-L-phenylalanine. The functionalization process is very simple and does not require complex equipment. Also, due to its compatibilty with biological materials such as tissues, it is usually employed for drug delivery purposes.

Though the study of PDA is an emerging area of interest and a wide range of its applications have been identified, its chemical structures are not well understood. The function and properties of PDA are influenced by reaction conditions such as the solvent, pH, and the concentration of dopamine HCl. Hence, to better understand its functionality in the different fields identified, its chemical structures need to be well studied. Analytical tools such as Fourier transform infrared spectroscopy and mass spectrometry are used to study the chemical structures of PDA. Furthermore, different chemical structures of the PDA have been proposed in literature based on the condition under which PDA is synthesized and the analytical tools that are employed. Based on the complex nature of the PDA, subjecting it to degradation and using different analytical tools for its studies also provide relevant information.

In this study, Deborah Takyibea Okyere, a Microelectronics-Photonics student working under the auspices of Dr. Jingyi Chen of the Department of Chemistry and Biochemistry, conducted a time-course study to understand the chemical structures formed during PDA formation and degradation to better understand the functionality of PDA used as a surface coating.

Appendix B: Executive Summary of Newly Created Intellectual Property

The new intellectual property created in the course of this research project and should be considered from both a patent and commercialization perspective.

1. Time course study approach employed in the synthesizing and degradation of PDA and used together with different analytical tools to understand the chemical sturcutres of PDA.

Appendix C: Potential Patent and Commercialization Aspects of Listed Intellectual Property Item

C.1 Patentability of Intellectual Property (Could Each Item be Patented)

The patentability of item listed under intellectual property was considered.

1. There is no standard method for the preparation of PDA for the purpose of characterizing and analyzing the chemical structures of PDA. The existing preparatory methods can be modified at any time to suit the studies being carried. Hence, the time course study approach employed can not be patent.

C.2 Commercialization Prospects (Should Each Item Be Patented)

1. Not applicable

C.3 Possible Prior Disclosure of IP

1. Not applicable

Appendix D: Broader Impact of Research

D.1 Applicability of Research Methods to Other Problems

Characterization methods such as Fourier transform infrared spectroscopy employed in this work can be used to study the chemical structures of organic compounds as well as metal-based nanoparticles such as silver and gold. Also, the dispersion method used for the synthesis of PDA can be used for surface functionalization purposes to coat diverse nanomaterials such as silica and silver with PDA.

D.2 Impact of Research Results on U.S. and Global Society

Research has shown that PDA has unique properties such as strong adhesive properties, compatibility to biological systems with little cytotoxicity, and chemical functionalities. Hence these features make the studies of PDA in applied fields such as biomedicine and catalysis very promising. For example, the adhesion property is most widely employed in coating the surface of nanoparticles such as gold, which serves as a stage for drug delivery and carrier for antibodies used in binding to antigens of interest. The result of this work would help in fine-tuning the application of PDA in the field such as biomedicine to optimize its functionality in drug delivery.

D.3 Impact of Research Results on the Environment

The preparation of PDA is simple, and materials used in its preparation do not have any adverse effect on the environment. However, depending on the field of application, PDA synthesized under different reaction conditions can have adverse effect on the environment. For example, the use of different concentration of dopamine in the synthesis of PDA can affect the release of drug from PDA platform. This may lead to side effects that are not desirable in humans.

Appendix E: Microsoft Project for MS MicroEP Degree Plan

	Spring 2019			
	Classes	**84 days?**	**Mon 1/14/19**	**Thu 5/9/19**
	MEPH 5911 -OP SEM: PERSONNEL MGMT	84 days	Mon 1/14/19	Thu 5/9/19
	MEPH 5383 - COMMERCIALIZING RESEARCH	84 days	Mon 1/14/19	Thu 5/9/19
	ELAC 0011 - GRAMMAR THROUGH EDITING	84 days	Mon 1/14/19	Thu 5/9/19
	PHYS 5613 - BIOPHYSICS & BIOPHYSICS TECHNIQUES	84 days	Mon 1/14/19	Thu 5/9/19
	Research	**93 days?**	**Wed 1/2/19**	**Fri 5/10/19**
	Finding a supervisor	1 day	Wed 1/2/19	Wed 1/2/19
	Finding a research topic	13 days	Mon 2/11/19	Wed 2/27/19
	PDA synthesis and characterization	66 days	Fri 2/8/19	Fri 5/10/19
	Synthesis of nanocubes and nanocages	50 days	Mon 3/4/19	Fri 5/10/19
	Committee Formation	11 days	Mon 3/4/19	Mon 3/18/19
	Summer 2019			
	Classes	**60 days?**	**Mon 5/13/19**	**Fri 8/2/19**
	MEPH 5821 - ETHICS FOR SCI AND ENG	45 days	Tue 5/28/19	Mon 7/29/19
	MATH 2554 - CALCULUS 1	38 days	Tue 5/28/19	Thu 7/18/19
	CHEM 600V - MASTER'S THESIS	54 days	Tue 5/28/19	Fri 8/9/19
	Research	**70 days**	**Mon 5/13/19**	**Fri 8/16/19**
	Silica conjugated to RNA for early detection of TB studies	70 days	Mon 5/13/19	Fri 8/16/19
	For Tribological studies of PTFE : a) Synthesize silica coated with polydopamine nanoparticles b. Synthesize copper nanoparticles coated with silica nanoparticles	70 days	Mon 5/13/19	Fri 8/16/19
	Fall 2019			
	Classes	**84 days**	**Mon 8/26/19**	**Thu 12/19/19**
	CHEM 5443 - PHYSICAL CHEM OF MATERIALS	84 days	Mon 8/26/19	Thu 12/19/19
	ELEG 5203 - SEMICONDUCTOR DEVICES	84 days	Mon 8/26/19	Thu 12/19/19
	MEPH 6811 -OP SEM : MGMT/LEADERSHIP	84 days	Mon 8/26/19	Thu 12/19/19
	ELAC 5043 - RESEARCH WRITING STEM	84 days	Mon 8/26/19	Thu 12/19/19
	Research	**84 days?**	**Mon 8/26/19**	**Thu 12/19/19**
	Synthesis of polydopamine and analyzing with mass spectrometer	85 days	Mon 8/26/19	Fri 12/20/19
	Synthesis of Silica coated with PDA for Tribology studies	85 days	Mon 8/26/19	Fri 12/20/19
	Synthesis of copper coated with silica/ copper-silica core-shell coated with PDA for Tribology studies	85 days	Mon 8/26/19	Fri 12/20/19
	Synthesis of silica coated with copper for Tribology studies	85 days	Mon 8/26/19	Fri 12/20/19
	Title form submitted to Graduate School	1 day	Fri 12/13/19	Fri 12/13/19
	Spring 2020			
	Classes	**84 days**	**Mon 1/13/20**	**Thu 5/7/20**
	MEPH 5611 - RESEARCH COMMUNICATION SEMINAR	84 days	Mon 1/13/20	Thu 5/7/20
	BMEG 5523 - BIOMED DATA AND IMAGE ANALYSIS	84 days	Mon 1/13/20	Thu 5/7/20
	MEPH 6911 - OP SEM.: ADV. MANAGEMENT AND LEADERSHIP	84 days	Mon 1/13/20	Thu 5/7/20
	CHEM 600V - MASTER'S THESIS	84 days	Mon 1/13/20	Thu 5/7/20
	MATH 2564C - CALCULUS 2	84 days	Mon 1/13/20	Thu 5/7/20
	Research	**85 days?**	**Mon 1/13/20**	**Fri 5/8/20**
	Analyzing synthesized polydopamine and its degraded products with nuclear magnetic resonance spectroscopy	85 days	Mon 1/13/20	Fri 5/8/20
	Silica conjugated to antibody for early detection of TB studies	85 days	Mon 1/13/20	Fri 5/8/20
	Synthesizing silica coated with silver for tribology studies	85 days	Mon 1/13/20	Fri 5/8/20
	Literature survey on PDA and Copper nanoparticles	49 days	Mon 3/23/20	Thu 5/28/20
	Summer 2020			
	Classes	**60 days?**	**Mon 5/11/20**	**Fri 7/31/20**
	MEPH 5832 - PROPOSAL WRITING AND MANAGEMENT	49 days	Tue 5/26/20	Fri 7/31/20
	MATH 2574 -Calculus III	38 days	Tue 5/26/20	Thu 7/16/20
	Research	**70 days?**	**Mon 5/11/20**	**Fri 8/14/20**
	Sythesis and characterization of copper nanoparticles coated with PEG-COOH and PEG-SH	70 days	Mon 5/11/20	Fri 8/14/20
	Copper/silver galvanic replacement	70 days	Mon 5/11/20	Fri 8/14/20
	Copper/ gold galvanic replacement	70 days	Mon 5/11/20	Fri 8/14/20
	Thesis introduction	70 days	Mon 5/11/20	Fri 8/14/20
	Fall 2020			
	Classes	**84 days**	**Mon 8/24/20**	**Thu 12/17/20**
	MEMS 5263 - Introduction to MEMS	84 days	Mon 8/24/20	Thu 12/17/20
	MSEN 5811 - Infrastructure Management	84 days	Mon 8/24/20	Thu 12/17/20
	MATH 2584C - Elementary Differential Equations	84 days	Mon 8/24/20	Thu 12/17/20
	Research	**84 days?**	**Mon 8/24/20**	**Thu 12/17/20**
	Analyzing of synthesized polydopamine and its degraded products with Fourier transform infrared spectroscopy and mass spectrometry	84 days	Mon 8/24/20	Thu 12/17/20
	Copper/gold galvanic replacement	84 days	Mon 8/24/20	Thu 12/17/20
	Spring 2021			
	INEG 5333 - Design of Industrial Experiments	79 days	Mon 1/11/21	Thu 4/29/21
	Thesis Writing and Copper Synthesis and Characterization Research	79 days	Mon 1/11/21	Thu 4/29/21
	Summer 2021			
	Research	63 days	Mon 5/10/21	Wed 8/4/21
	National Science Foundation I-Corps Program	33 days	Tue 6/8/21	Thu 7/22/21
	Fall 2021			
	Class	**85 days**	**Mon 8/23/21**	**Fri 12/17/21**
	MSEN 5313 - Fundamentals of Material Science	85 days	Mon 8/23/21	Fri 12/17/21
	Research	**100 days**	**Mon 8/2/21**	**Fri 12/17/21**
	Research - Antimicribial and Anti-viral project	100 days	Mon 8/2/21	Fri 12/17/21
	End Game			
	Professor starts corrections to completed final draft paper	25 days	Tue 5/11/21	Mon 6/14/21
	Last day to send all Abstract, Title, and Scheduling to MicroEP office	1 day	Mon 6/14/21	Mon 6/14/21
	Last day for Major Professor's Final Approval	2 days	Mon 6/14/21	Tue 6/15/21
	Last Day for MicroEp QC Approval before sending to Committee	2 days	Thu 6/17/21	Fri 6/18/21
	Public Defense	1 day	Fri 6/18/21	Fri 6/18/21
	Defense	1 day	Fri 6/25/21	Fri 6/25/21
	Final Correction	69 days	Mon 6/28/21	Thu 9/30/21
	Last day to Apply for Fall 2021 Graduation	1 day	Fri 10/1/21	Fri 10/1/21
	Submission of Thesis to Graduate School	1 day	Thu 10/14/21	Thu 10/14/21
	Commencement	1 day	Sat 12/18/21	Sat 12/18/21

Appendix F: Identification of All Software Used in Research and Thesis Generation

Computer #1:
Model Number: A1398 EMC 2876
Serial Number: C02PF1QVG3QC
Location: Personal Laptop
Owner: Deborah Takyibea Okyere
Software #1:
Name: Microsoft 356 Apps for enterprise
Purchased by: Electrical Engineering Department, University of Arkansas
Software #2:
Name: Adobe Creative Cloud
Purchased by: Electrical Engineering Department, University of Arkansas
Software #3:
Name: ChemDraw 20.0
Purchased by: Department of Chemistry and Biochemistry
Software #4:
Name: TopSpin 32
Purchased by: Department of Chemistry and Biochemistry
Software #5:
Name: OriginPro 2021 (Student version)
Serial Number: GA354 6089 7175117
Purchased by Sylvester Amoah
Software #6:
Name: FlexAnalysis Version 3.4 (Build 135) for data acquisition and FlexAnalysis Version 3.4 (Build 76) for data analysis
Purchased by: University of Arkansas Statewide Mass Spectrometry Facility

Appendix G: All Publications Published, Submitted and Planned

G.1. Articles in Refereed Journals

1. Soltani-Kordshuli, F.; Okyere, D.; Chen, J.; Miller, C.; Harris, N.; Afshar-Mohajer, M.; Ghosh, S.K.; Zou, M., Tribological behavior of the PDA/PTFE + Cu-SiO_2 nanoparticle thin coatings. *Surface and Coatings Technology* **2021,** 409, 126852.

2. Niyonshuti, I.I; Krishnamurthi, V. R.; Okyere, D.; Song, L.; Benamara, M.; Tong, X.; Wang, Y.; Chen, J. Y., Polydopamine Surface Coating Synergizes the Antimicrobial Activity of Silver Nanoparticles. *ACS Applied Materials & Interfaces* **2020,** *12* (36), 40067-40077.